applied sciences

MDPI

Review

Analysis of Photosynthetic Systems and Their Applications with Mathematical and Computational Models

Shyam Badu [1], Roderick Melnik [1,2] and Sundeep Singh [1,*]

[1] MS2Discovery Interdisciplinary Research Institute, Wilfrid Laurier University, 75 University Avenue West, Waterloo, ON N2L 3C5, Canada; sbadu@wlu.ca (S.B.); rmelnik@wlu.ca (R.M.)

[2] BCAM-Basque Center for Applied Mathematics, Alameda de Mazarredo 14, E-48009 Bilbao, Spain

* Correspondence: ssingh@wlu.ca

Received: 30 August 2020; Accepted: 25 September 2020; Published: 29 September 2020

Abstract: In biological and life science applications, photosynthesis is an important process that involves the absorption and transformation of sunlight into chemical energy. During the photosynthesis process, the light photons are captured by the green chlorophyll pigments in their photosynthetic antennae and further funneled to the reaction center. One of the most important light harvesting complexes that are highly important in the study of photosynthesis is the membrane-attached Fenna–Matthews–Olson (FMO) complex found in the green sulfur bacteria. In this review, we discuss the mathematical formulations and computational modeling of some of the light harvesting complexes including FMO. The most recent research developments in the photosynthetic light harvesting complexes are thoroughly discussed. The theoretical background related to the spectral density, quantum coherence and density functional theory has been elaborated. Furthermore, details about the transfer and excitation of energy in different sites of the FMO complex along with other vital photosynthetic light harvesting complexes have also been provided. Finally, we conclude this review by providing the current and potential applications in environmental science, energy, health and medicine, where such mathematical and computational studies of the photosynthesis and the light harvesting complexes can be readily integrated.

Keywords: photosynthetic systems; light harvesting complexes; Fenna–Matthews–Olson (FMO); bacteriochlorophyll (BChl); density functional theory (DFT); molecular dynamics; artificial photosynthesis; biomimetic and synthetic biology; sustainability; quantum biology; green economy; time-dependent phenomena

1. Introduction

Photosynthesis is a process by which green plants and certain other organisms convert light energy into chemical energy which is then served as an energy source for all forms of life. A common example of the photosynthesis process is the conversion of carbon dioxide (CO_2) and water (H_2O) into the carbohydrate and oxygen in the presence of sunlight in plants. This type of photosynthesis is known as oxygenic photosynthesis which occurs in, among others, eukaryotic microorganisms such as algae and in bacteria such as cyanobacteria. There is also another type of photosynthesis, which is known as anoxygenic photosynthesis that does not produce oxygen and is used by other bacteria such as the purple bacteria, the green sulfur and nonsulfur bacteria, as well as by the acidobacteria and the heliobacteria. Significant research efforts have been devoted on using photosynthetic organisms or mechanisms as a source to produce clean, cheap and renewable energy [1]. The photosynthetic process is first initiated by the absorption of sunlight by the light harvesting complexes resulting in

the generation of electronically excited state being subsequently transferred to the reaction centre where charge separation occurs. Notably, this transfer of energy is facilitated by the pigment-protein complexes, such as light harvesting complex II, CP26 and CP29 in green plants and algae, as well as model organisms of green sulfur bacteria such as Chlorobium tepidum and Fenna–Matthews–Olson (FMO) complex [2]. The structures of both the light harvesting II and FMO complexes as determined by the X-ray crystallography show that such complexes are built from a network of chromophore molecules, such as bacteriochlorophyll (BChl) *a* [2–4]. In addition to being important for the plants, the photosynthetic systems are also being used for the production of bioactive compounds, as well as in biomedicine [5–7]. One such example is the application of the photosynthetic bacteria in the purification of waste water and biomass recovery that has been experimentally demonstrated in [8].

Green sulfur bacteria are photoautotrophic inhabitants of aquatic anoxic environments that possess a unique and complex photosynthetic machinery which permits them to thrive in an oxygen-free, sulfur-rich and often light-limited environment [9,10]. In photosynthetic green sulfur bacteria, the specialized light-absorbing green pigments called chlorophyll absorbs the light photons that are further transferred through a water-soluble pigment-protein complex known as FMO to the reaction center to drive the charge separation [3]. Owing to the important role played by the FMO complex in the energy transfer in green sulfur bacteria, significant research efforts have been made in the past decade for our better understanding of their optical properties utilizing a wide range of spectroscopic and theoretical approaches, making it an ideal protein model system for studying exciton dynamics and excitation energy transfer in the photosynthetic complexes [3,4,11–16]. In particular, we recall that the FMO protein complex contains seven BChl *a* molecules wrapped in a string bag of protein that plays an important role in green sulfur bacteria, connecting the chlorosome antenna to the reaction center where the photosynthesis events occur. Experimentally, the eighth BChl pigment has also been newly resolved in the FMO protein that lies perpendicular to the plane of the other seven BChls [17,18]. Notably, FMO complex is a homotrimer of three $\approx$ 40 kDa monomer that possesses C3 symmetry whereby three copies of each subunit of seven BChl *a* chromophores bind together to the eighth BChl *a* pigment [16,19,20]. Due to close packing of BChl *a* pigments in each monomer subunit, the excited electronic states of FMO complexes are delocalized over multiple pigments. The previous research in this field is mainly focused on developing and testing new computational and experimental methods for a better understanding of the delocalization of excited states over multiple pigments and the unfolding of the relationship between atomic structure and absorbance along with the fluorescence spectra [19,20]. Owing to the rotational symmetric of the monomer subunit of FMO trimer around the symmetry axis, there are two types of FMO complex structures widely analyzed in the literature. The first structure comprises of only a single monomer of protein complex given by the pdb code 3EOJ [17,18]. Another structure available in the protein data bank is the 3ENI which exists as a dimer of the protein complex with each monomer having eight BChl pigments [21]. The difference between these structures lies in the fact that the former is taken from the species Prosthecochloris aestuarii with the resolution of 1.3 Å and the latter is from the species Chlorobium tepidum with the resolution of 2.3 Å. The structure of FMO complex including the entire protein taken from protein data bank (3ENI) is shown in Figure 1a and the corresponding model without protein is shown in Figure 1b. There are also some other structures of the FMO protein taken from the Chlorobium tepidum [22].

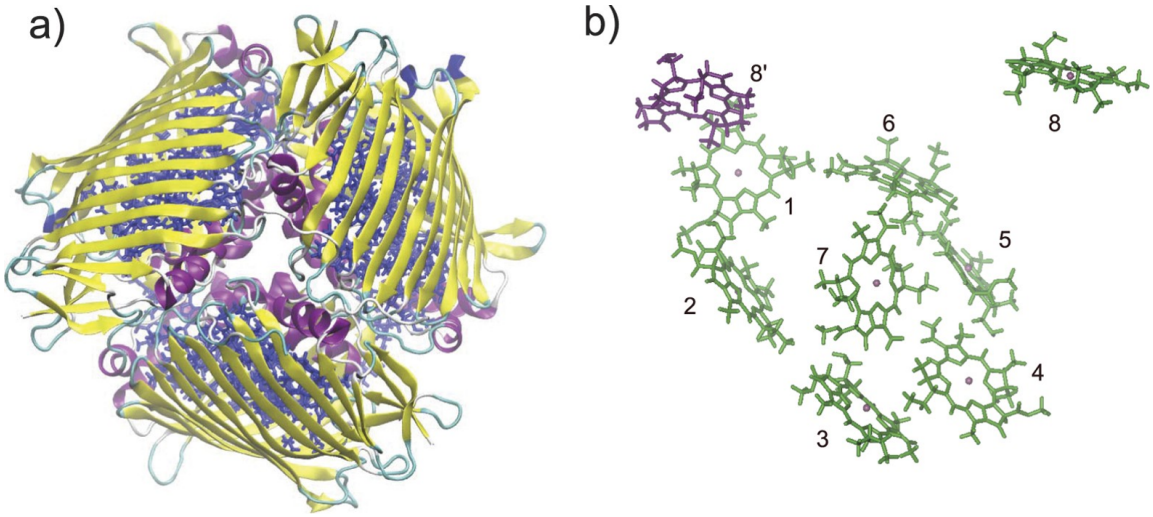

Figure 1. (Color online) (**a**) the FMO trimer structure from C. tepidum (PDB ID: 3ENI) demonstrating the packing of BChls (colored in blue) inside the protein backbone (colored yellow), and (**b**) the spatial arrangement of BChls taken out from the protein pocket. The eight BChls of the same monomer are colored in green while the BChl 8′ of the nearest–neighboring monomer is colored in purple. (This figure is reproduced from [23] under the terms of the creative commons attribution 4.0 International License (http://creativecommons.org/licenses/by/4.0/), Copyright © 2020, Springer Nature)

Many experimental and computational studies have been reported on the structure of chlorophyll utilizing the density functional theory (DFT) and nuclear magnetic resonance (NMR) techniques (including solid-state and liquid-state NMR) for understanding its role in the photosynthesis process [24–29]. Calculation of the electronic g-tensors of the semiquinone active sites of photosynthetic reaction centers in a variety of protein environments using DFT has also been reported in [30]. Furthermore, calculation of the nuclear quadrupole parameters has been performed on the chlorophyll *a* [31], but no such a systematic computational study for the BChl has been reported till now. Hence, the calculation of these parameters on the BChl of FMO protein is an important subject to study. We also note that the quantum coherence studies of the FMO complex have been reported in a number of works to elucidate the quantum mechanical time-dependent phenomenon associated with the process of photosynthesis [32–42]. Moreover, the mutation of the FMO light harvesting complex can cause changes in the observed phenomenon of quantum coherence. In some of the studies, the effect of the mutation has also been studied by conducting the site-specific mutagenation for the FMO complex and accordingly its absorption spectra and circular dichroism has been reported and analyzed [43–45]. It is well-known that apart from the absorption of light from the sun, the light harvesting complexes are also responsible for maintaining the energetic state and chemical state of the complexes available in the photosynthetic reaction center. The parts of the light harvesting complex systems that control the reaction center's chemical and energetic state are known as the quenchers such as carotenoids. Although such quenchers are not available in the FMO protein, it has been experimentally found that the cysteine residues located near the low-energy BChls are responsible for regulating the effective energy transfer in aerobic conditions in the reaction center of green sulfur bacteria [46,47]. A complete elucidation and better understanding of the associated phenomena would significantly assist in the design of bio-inspired light harvesting antennas along with the redesign of the natural photosynthetic systems [47].

The infrared spectra of the chlorophylls *a*, *d* and *f* have been calculated using modern density functional (CAM-B3LYP) and high-level symmetric adapted coupled cluster configuration interaction (SAC-CI) in [48]. The effect of magnesium ligation on the geometry and spin density distribution of the cation free radicals have also been quantified in the models of chlorophyll and BChl using DFT in [49]. This study reported that there is a formation of the radical orbitals without significant changes in the

hyperfine coupling of the systems. It has also been noted that the energy transfer phenomenon in the FMO complex is well described by solving the hierarchical equations of motion for such systems [50–54]. The potential energy surface for the BChl pigments taken from the FMO complex has also been computed using a combination of molecular dynamics and quantum mechanics simulations [55]. A more detailed description of such computational methods and their advancements in this field of research has been elaborated in [56]. The excitonic energy transfer for the biological systems related to the photosynthesis phenomenon, i.e., the biological chromophore and light harvesting complexes, can be evaluated using the path integral dynamics as highlighted in [57–59]. Furthermore, the normal mode analysis of the spectral density has been studied using the time-dependent DFT in [60] for computing the spectral densities due to coupling between light harvesting pigments and their corresponding protein. This method is a combination of the charge density coupling and the transition charge density electrostatic potential with the normal modes of the protein pigment that is studied via correlation in the site energies of the complex, as well as the scheme of its returning from the coherence state to the original state.

Several advances have been reported on the computational study of the FMO complex, using molecular dynamics simulation as well as the DFT to study its spectral density, excitation energy and optical spectra [61–66]. The comparative study for the excited energy distribution and spectral density of the two different kinds of light harvesting complexes, i.e., PE545 photosynthetic complex and FMO complex, has been done utilizing molecular dynamics simulation along with the quantum mechanical calculations incorporating the environment of the complexes in [67,68]. These studies are also supporting the existence of quantum coherence which is a subject of continuing debate [69–76]. The study of pump-probe polarization phenomena of the photosynthetic light harvesting complexes has also been reported in the previous works for several kinds of coherences and the long-time vibronic coherences have been observed in the FMO [77–79]. The electron-nuclear interaction in the BChl systems of the FMO complex has also been described in a molecular dynamics-based study of [80], which also signifies the influence of electronic relaxation caused by the environmental changes. Significant efforts have been devoted for studying the light harvesting complex II and the FMO complex for quantifying the correlation between the energies of different pigments existing in the FMO protein [81,82]. The pathways for the energy transfer between different pigments of the FMO complex have also been previously studied by using a combination of the quantum mechanical and molecular dynamics simulations. By knowing the direction of energy transfer between different pigments of FMO, one could easily find out their excitation which ultimately depends on the position of these pigments [23,44,83]. Further analysis of the energy transfer and the spectroscopic properties would considerably help in the development of more refined models in this research field [44].

This review includes different exciting applications of photosynthesis phenomena in the ecosystems, environmental sciences and biomedicine. In this context, we will also highlight some of the most recent developments in the mathematical and computational modeling of FMO complexes. In particular, we will review recent results on spectral density, quantum coherence, quantum entanglement and excitonic energies of different pigments in the light harvesting complexes. We will also discuss the issues pertinent to the highest occupied orbital (HOMO) and lowest unoccupied orbital (LUMO) energies for all the BChls utilizing the time-dependent DFT. These results would be helpful in studying the excitonic dynamics of the light harvesting complexes among different applications. Hence, we will focus on reviewing the energetic and spectroscopic properties of different types of BChls computed using DFT.

The rest of this paper is organized as follows: in Section 2, we will discuss some of the most suitable types of theoretical and computational techniques used to calculate the properties of the photosynthetic light harvesting complexes. The results of the recent time-dependent DFT calculations on the FMO complex are presented and discussed in Section 3. In Section 4, we describe current and potential applications of the development of mathematical and computational techniques for photosynthesis and light harvesting complexes. Concluding remarks and outlook are given in Section 5.

2. Methodology

In this section, we shall describe some of the most applicable computational and theoretical techniques used to calculate the pertinent physical properties of the photosynthesis-based systems and phenomena of FMO light harvesting complex found in the green sulfur bacteria, viz., site energy, spectroscopic properties and spectral densities. In addition, the nuclear quadruple properties of the FMO complex and other light harvesting complexes will also be discussed.

2.1. Calculation of Nuclear Magnetic Resonance (NMR) and Nuclear Quadrupole Resonance (NQR) Properties

Nuclear magnetic resonance (NMR) spectroscopy has been long investigated to provide the atomic-scale and element-specific detailed information about the structure, disorder and dynamics of materials [84]. In photosynthetic antenna complexes, solid-state NMR has significantly assisted in providing a mechanistic and electronic perspective of the pigment–protein and pigment–pigment interactions by resolving their atomic details [85]. Several structures of the photosynthetic membrane proteins have been resolved in the past decades using high resolution crystallography. However, in depth details of the structure–function interactions of photosynthetic membrane proteins still remain to be elucidated, which can be resolved using the solid-state NMR [85]. NMR spectra of quadrupolar nuclei are often challenging due to the associated anisotropic (or orientation-dependent) interactions, including chemical shift anisotropy and dipolar coupling. Notably, solid-state NMR spectroscopy of quadrupolar nuclei has been widely used in diverse problems related to chemistry, biology, geology, and materials science. Thus, it becomes extremely crucial to develop the methods for studying these nuclei to exploit their site-specific and atomic-scale structural information using NMR spectroscopy [84]. The NMR and NQR spectra for a BChl monomer taken from the FMO complex can be easily computed utilizing the computational approaches [86], whereby the chemical shifts that represent the change of resonance frequency of nucleus relative to a given standard are generally measured. This chemical shift of a nucleus that plays a vital role in the structural characterization of molecules is related to the shielding tensors as [86]:

$$\delta = 1\sigma_{iso} - \sigma, \tag{1}$$

where σ is the shielding tensor which describes the magnetic polarizability of an atomic nucleus under study, 1 is the unit matrix and σ_{iso} is the isotropic value or trace of the shielding tensor of the standard reference used in the NMR experiments. Mathematically, the shielding tensor (also known as absolute chemical shift) is defined by the following relation [86]:

$$\sigma_{\alpha\beta} = \left(\frac{\partial^2 E}{\partial \mu_\alpha \partial B_\beta} \right), \tag{2}$$

where $\alpha, \beta = 1, 2, 3$ are the tensor indices, E is the total electronic energy of the molecule, B is the external magnetic field and μ is the magnetic moment of the nucleus of interest. In calculating the chemical shift, the difference between the measured shielding tensor and the shielding tensor of the reference system is obtained. The tetra methyl saline (TMS) has been taken as a reference system (see, e.g., [86]). Furthermore, the value of the isotropic shielding coefficient can be computed by averaging the three principal components of shielding tensor obtained from the shielding tensor matrix, i.e., $\sigma_{iso} = (\sigma_{11} + \sigma_{22} + \sigma_{33})/3$. Moreover, another quantity that describes the electronic structure properties of the system is known as the nuclear quadruple interaction. Calculations of the quadruple interaction properties such as the asymmetry parameter and quadruple frequency for the nuclei ^{14}N and ^{25}Mg available in each BChl of FMO complex can also be done.

If V_{XX}, V_{YY} and V_{ZZ} are the principal components of the electric field gradient (EFG) tensors, then the asymmetry parameter of the system can be expressed as [87]:

$$\eta_Q = \frac{V_{YY} - V_{XX}}{V_{ZZ}}, \tag{3}$$

where symbol Q stands for the nuclear quadruple moment and the EFG tensor follow the order

$$|V_{ZZ}| \geq |V_{YY}| \geq |V_{XX}|, \tag{4}$$

and the EFG tensor is traceless, i.e.,

$$\sum_i V_{ii} = 0. \tag{5}$$

From the above relations, one can easily express:

$$V_{XX} = -\frac{1}{2}(1 + \eta_Q)V_{ZZ}, \tag{6}$$

$$V_{YY} = -\frac{1}{2}(1 - \eta_Q)V_{ZZ}. \tag{7}$$

Furthermore, the quadruple coupling constant can be obtained from the values of the electric field gradient tensor and quadruple moment of the nuclei as

$$C_Q = \frac{1}{h}eQeq \quad ; \quad eq = V_{ZZ}, \tag{8}$$

where, as before, Q is the nuclear quadruple moment of the nuclei under study which is expressed in the unit barn, h is Planck's constant and e is the electronic charge. Next, we will describe the mathematical formulation for computing the energy density of light harvesting complexes arising from excited states.

2.2. Quantum Entanglement

In the explanation of quantum mechanical phenomena associated with the light harvesting complexes, the accurate characterization of the energy of one system cannot be described without taking into account the other energy states. The key phenomenon of this type is known as quantum entanglement and is particularly important to be considered for the chlorophyll pigments or chromophores present in the reaction centers of light harvesting complex [88–90]. The formulation of the quantum entanglement for the FMO complex as described here has been adopted from [88]—whereby the state in the single-excitation manifold of the light harvesting complex can be expressed as [88]

$$\rho(t) = \sum_{i=1}^{N} \rho_{ii}(t)|i\rangle\langle i| + \sum_{i=1}^{N}\sum_{j>i}^{N} \rho_{ij}(t)|i\rangle\langle j| + \rho_{ij}^*(t)|j\rangle\langle i|, \tag{9}$$

where $\langle i|$ represents the state for which only the ith chromophore (site) is excited and all other chromophores are in their electronic ground states and ρ is an unnormalized density matrix of N chromophores. Furthermore, the mixed-state entanglement in the physically relevant zero- and single-excitation subspaces of the light harvesting complexes can be readily computed from [88]:

$$E[\rho] = -\sum_{i=1}^{N} \rho_{ii} \ln \rho_{ii} - S(\rho), \tag{10}$$

where the quantity $S(\rho)$ is known as the von Neumann entropy of the state ρ and is given by the relation: $S(\rho) = -\mathrm{tr}(\rho \ln \rho)$ [91].

Moreover, the analysis of physical structure and energy levels of FMO complex indicates that sites 1 and 6 interface with the chlorosome, transmitting energy to the complex, and experiments have

also confirmed that sites 1 and 6 are the first to become excited in the FMO protein [3,88]. The global quantum coherence in the FMO protein at two different temperatures, viz., 77 K (commonly employed temperature for the ultrafast spectroscopy experiments in probing the light harvesting complexes) and physiologically relevant temperature of 300 K, has been presented in Figure 2. This study demonstrates the direct implementation of Equation (10) for the initial state excitation on site $|1\rangle$ or $|6\rangle$ (see further details in [88]). As depicted in Figure 2, the general feature of the global entanglement measure for all scenarios is that its value rises rapidly for short times due to the quick delocalization of the excitation caused by large 1–2 and 5–6 site coupling terms in the Hamiltonian of FMO complex and then decays after approximately 30–50 fs with varying amounts of oscillation as the excitation begins to explore other sites owing to incoherent transport and rapid dephasing. Furthermore, there is finite entanglement in the system up to 5 ps for both initial conditions and temperatures.

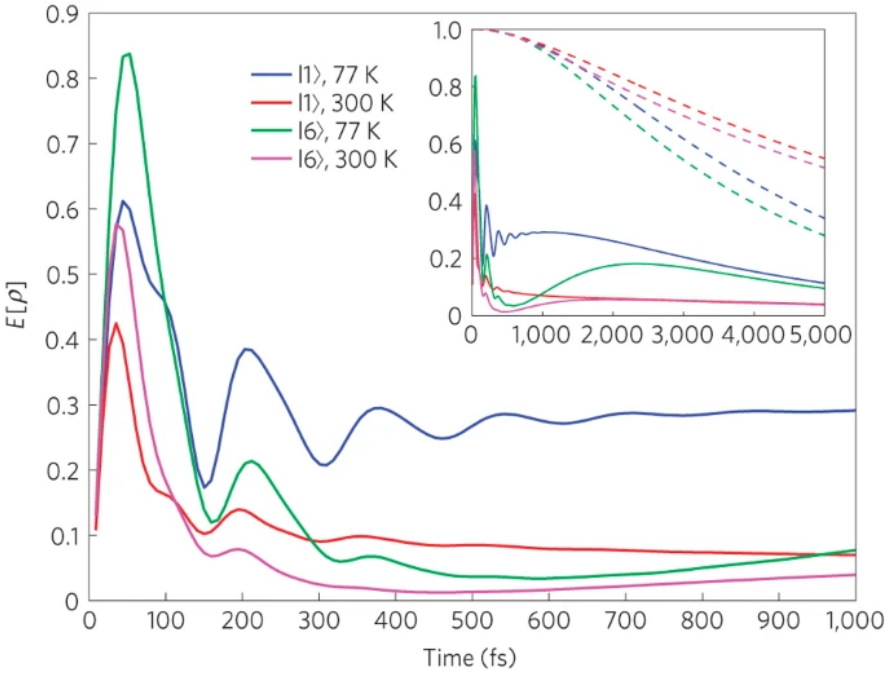

Figure 2. (Color online) Time evolution of the global quantum entanglement for the two initial states $|1\rangle$ and $|6\rangle$ at low (77 K) and high (300 K) temperatures for the FMO protein. The inset shows the long-time evolution of the same quantities, together with the trace of the single-excitation density matrix represented by the dashed lines with identical colour coding and the same units on the main axes). (This figure is reproduced with permission from [88])

In reality, the quantitative value of the unnormalized density matrix ρ determines the amount of entanglement in the respective state. This quantum entanglement observed between the different sites or the chromophores or the BChls in the FMO complex might explain the existence of correlations between them that can be clarified utilizing the quantum mechanics approach, which has become a very important tool for analyzing a range of phenomena observed in biological systems. The quantity ρ (the density matrix of the system in the basis of local excited states given in Equation (9) determines whether two states generating this density matrix are separable or not. Furthermore, the quantum coherence observed between the different BChls present in the FMO light harvesting complex also reshuffles the energy distribution that will initiate the energy transfer among them [92]. It is noteworthy to mention that the importance of the quantum coherence in this context continues to be debated [74–76,93–97].

2.3. Hierarchical Equations of Motion (HEOM)

The hierarchical equations of motion (HEOM) plays an important role in studying the photosynthetic electronic energy transfer by quantifying the site-dependent reorganization dynamics of protein environments [53,98,99]. In particular, the HEOM theory has been extensively used to: (a) account for various linear and nonlinear spectra in molecular and solid state materials, (b) evaluate charge and exciton transfer rates in biological systems, (c) simulate resonant tunneling and quantum ratchet processes in nanodevices, and (d) explore quantum entanglement states in quantum information theories [100]. Notably, the electronic exciton dynamics in the light harvesting complexes are also coupled to the vibrations and other mechanical modes that could induce a possibility of the memory effects in this process. Prolonged coherent dynamics is predicted in the light harvesting complexes due to the slow dissipation of reorganization energy to the vibrational environment [53]. The HEOM and its solution provide a better way for understanding the excitation and energy transfer phenomena in the light harvesting complexes by also accounting for the nonlocal time effects [53,98,99,101,102]. Importantly, the excitation energies of each and every pigment or the sites of the FMO complex have to be determined for studying the excited state phenomenon based on the absorption of the light at different sites of the FMO protein. The study of excitonic dynamics of the different sites of the pigments in the FMO complex has been performed in [103]. The detailed theoretical analysis of electronic excitation energy transfer through the FMO pigment–protein complex has been provided in [104]. In the earlier studies, there were only 7 BChls reported for the FMO complex and, accordingly, the excitonic Hamiltonian was described by 7×7 matrix [50,53]. Moreover, there has also been experimental evidence for the existence of the eighth pigment in the FMO protein [17,18], thus the Hamiltonian for the system comprising of 8×8 matrix can be expressed as:

$$H_{FMO} = \begin{bmatrix} 12,405 & -87.7 & 5.5 & -5.9 & 6.7 & -13.7 & -9.9 & 21 \\ -87.7 & 12,530 & 30.8 & 8.2 & 0.7 & 11.8 & 4.3 & 42 \\ 5.5 & 30.8 & 12,210 & -53.5 & -2.2 & -9.6 & 6 & 0.6 \\ -5.9 & 8.2 & -53.5 & 12,320 & -70.7 & -17.0 & -63.3 & -1.3 \\ 6.7 & 0.7 & -2.2 & -70.7 & 12,480 & 81.1 & -1.3 & 33 \\ -13.7 & 11.8 & -9.6 & -17.0 & 81.1 & 12,630 & 39.7 & -7.9 \\ -9.9 & 4.3 & 6.0 & -63.3 & -1.3 & 39.7 & 12,440 & -9.3 \\ 21 & 42 & 0.6 & -1.3 & 3.3 & -7.9 & -9.3 & 12,430 \end{bmatrix} \quad (11)$$

Furthermore, the values of the site energies and their coupling during the photosynthetic excitation are calculated by using Equation (12) (see Section 2.4) by fitting the optical spectra from the excitonic coupling between different pigments of the FMO complex. The diagonal components of Equation (11) denote the site energies and the off-diagonal elements denote the coupling between different sites. Notably, the elements of the Hamiltonian matrix presented in Equation (11) have been determined by fitting the optical spectra obtained by utilizing experimentally determined shapes for the spectral densities. More details about the process of testing the Hamiltonian via calculation of the excitation spectra using experimental and computational techniques can be found in [50,103,105–107].

2.4. Calculation of Energies and Spectral Density of FMO Complex

In order to shed more light on the site energies and spectral density of the FMO complex, we recall the theoretical method used in [23], where a combination of quantum mechanical and molecular mechanics techniques have been used for computing them. Assuming that the quantities μ_k and μ_m are the strengths of the transition dipole moments for the kth and mth pigments, the coupling between the pigments can be expressed using the point dipole approximation as [23,108,109]:

$$V_{km} = f\frac{\mu_k \mu_m}{R_{km}^3}[\vec{\mu}_k \cdot \vec{\mu}_m - 3(\vec{\mu}_k \cdot \vec{n}_{km})(\vec{\mu}_m \cdot \vec{n}_{km})], \quad (12)$$

where f is the protein screening factor and R_{ij} is the distance between transition dipoles with the direction $\vec{n}_{km}$.

For quantifying the spectral density, the autocorrelation function for each pigment can be computed from:

$$C_k(t_i) = \frac{1}{M}\sum_{l=1}^{M}\left[\frac{1}{N-i}\sum_{j=1}^{N-i}\Delta E_{k,l}(t_i+t_j)\Delta E_{k,l}(t_j)\right], \tag{13}$$

where the quantity $\Delta E_{k,l}$ is the energy difference at time step t_i for the BChl k in monomer l, which is given by:

$$\Delta E_{k,l} = E_{k,l}(t_i) - \langle E_{k,l}\rangle, \tag{14}$$

where $E_{k,l}(t_i)$ is the instantaneous site energy and $\langle E_{k,l}\rangle$ is the mean value of site energy. Furthermore, the autocorrelation function ($C(t)$) is related to the spectral density ($J(\omega)$) via the fluctuation-dissipation theorem as:

$$C(t) = \frac{1}{\pi}\int_{\infty}^{\infty} d\omega \frac{e^{-i\omega t}J(\omega)}{1-e^{-\beta\omega}}, \tag{15}$$

where $J(\omega)$ is the spectral density and β is the inverse temperature denoted by $\beta = 1/(k_B T)$. Importantly, there are two different kinds of the models that can be used for spectral density ($J(\omega)$). One of them is the Drude model that can be expressed as [110]:

$$J(\omega) = \frac{2\gamma\lambda\omega}{\omega^2+\gamma^2}, \tag{16}$$

where λ denotes the reorganization energy that corresponds to the system-bath coupling strengths and γ is the cut-off frequency. The correlation function, approximated by a biexponential function with the Markovian white noise residue (WNR) ansatz, can be expressed as [110]:

$$C(t>0) \approx ce^{-\gamma t} + c'e^{-\gamma' t} + 2\Delta\delta(t). \tag{17}$$

The associated parameters can be obtained, as in [110], by exploiting the Laurent expansion and [1/1] Padé approximation as:

$$c = \frac{2\lambda}{\beta}\left[1 - 10(\beta\hbar\gamma/20)^2 - \frac{2.45}{(\gamma'/\gamma)^2-1}\right] - i\lambda\hbar\gamma, \tag{18}$$

$$c' = \frac{4.9\lambda\gamma\gamma'}{\beta(\gamma'^2-\gamma^2)}; \Delta = \beta\lambda\hbar\gamma/20. \tag{19}$$

Equation (17) combined with Equations (18) and (19) is used for fitting the correlation function and spectral density can be computed by substituting γ, γ' and λ into Equation (16).

If the nuclear motion of the BChl system is considered in the protein environment, then the excitation energy transfer can be described by normal coordinates and the displacement of the nucleus can be described by [80]: $\delta\epsilon^{\alpha} = \sum_i c_i^{\alpha} Q_i^{\alpha}$, where c_i^{α} and Q_i^{α} are the gradient of nuclear displacement and normal coordinates of the system, respectively. The spectral density of the system of the BChl can be computed by the determination of the correlation function. For providing better clarity, the computed results of BChl spectral density in [80] have been presented in Figures 3 and 4 utilizing various computational techniques. The spectra for the different kinds of BChls from the FMO complex for their mutated systems have been reported in [45]. Figure 5 presents the low temperature absorption spectra for eight different BChls from the FMO complex of their original and mutated states [45]. Such studies can assist in accurately modeling the process of energy transfer in the light harvesting complex by computing the absorption spectra of individual sites of the BChls. The mutation of the

FMO complex has also been done by focusing one by one on different sites, and more details about such mutogenation can be found in [45].

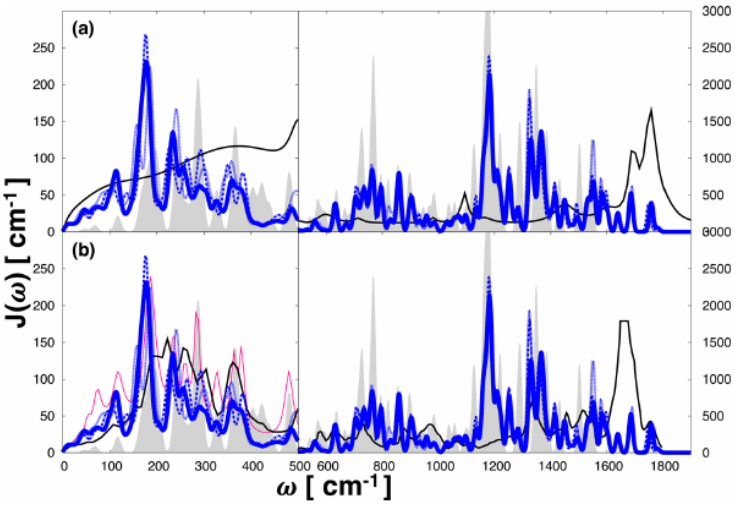

Figure 3. (Color online) Comparison of the spectral density calculations of a particular BChl 3 from the three different units of the FMO complex (FMO subunit A: solid line, FMO subunit B: dashed line and FMO subunit C: dot-dashed line) with the experimentally obtained data (represented by light-gray filled curve) extracted with the fluorescence line narrowing (FLN) measurements. The black curve represents the spectral density for BChl 3 computed using molecular dynamics excitation energy correlation function obtained with: (**a**) ZINDO/S-CHARMM protocol and (**b**) DFT-Amber protocol. The dark pink curve in (**b**) represents the low-frequency spectral density obtained from FLN experimental data (This figure is reproduced with permission from [80]).

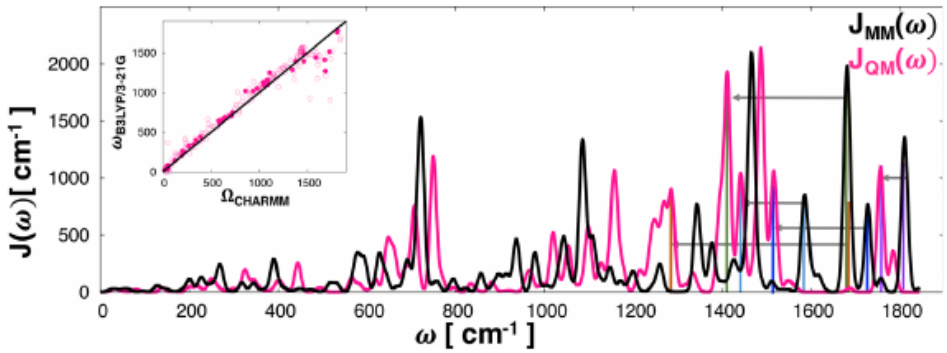

Figure 4. (Color online) Comparison of potential surface properties and the spectral density calculated from the ground state quantum mechanics surface vibrational frequency free state of the BChl and the molecular mechanics surface normal mode vibrational frequency in wavenumbers. (This figure is reproduced with permission from [80]).

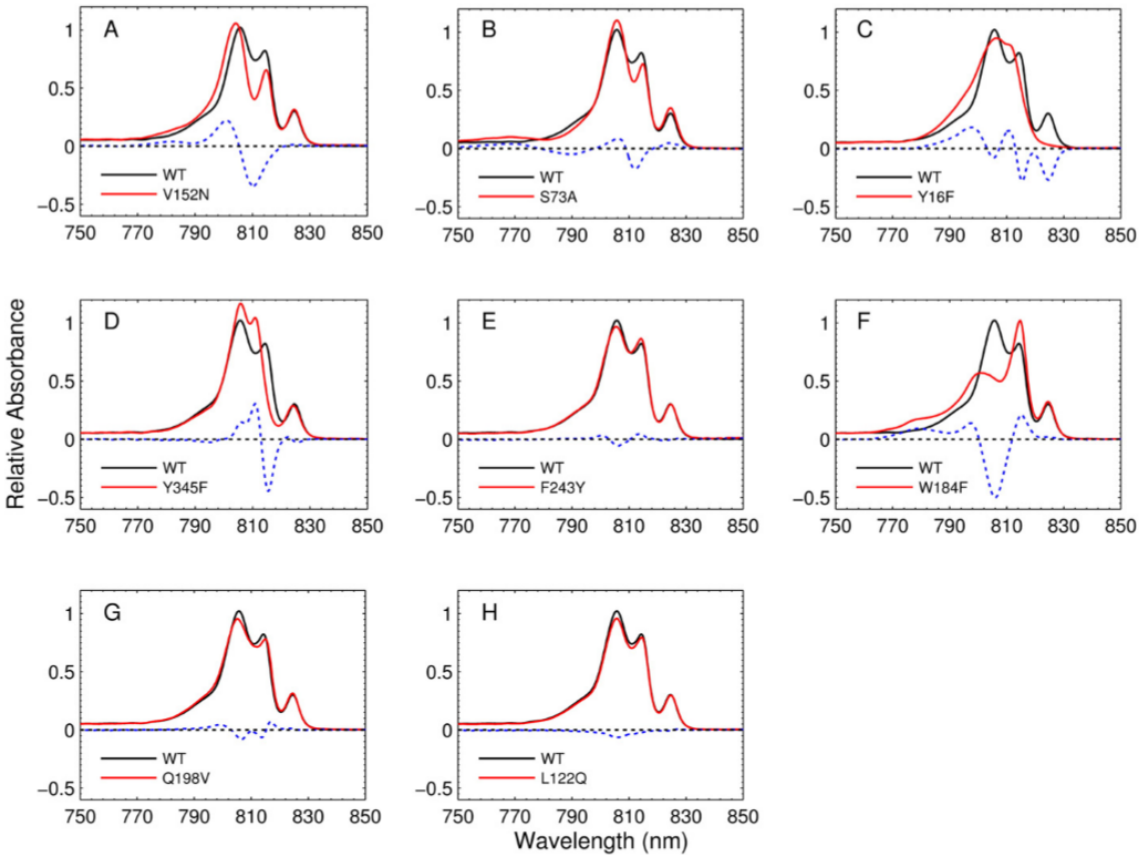

Figure 5. (Color online) Low temperature absorption spectra for the wild-type (WT) FMO complexes (black lines) and the mutants (red lines). (**A**–**H**) show the absorption spectra of FMO complexes carrying mutations in amino acid residues near BChls 1–8, respectively. The blue dashed lines represent the mutant minus wild-type absorption difference spectra. (This figure is reproduced with permission from [44]).

2.5. *Normal Mode Analysis*

Here, we will describe the mathematical formulation of the normal mode analysis following the procedure described in [60,111]. In order to perform the normal mode analysis associated with the spectral density of FMO light harvesting complex, first, we define a standard time-dependent Hamiltonian for the pigment-protein complex responsible for the light harvesting phenomena as [60]:

$$H = \sum_{mn} H_{mn}(t)|m\rangle\langle n| + \sum_{\xi} \frac{\hbar\omega_{\xi}}{4}(P_{\xi}^2 + Q_{\xi}^2), \tag{20}$$

where $|m\rangle$ represents a state where only pigment m is excited and all other pigments are in their electronic ground state, the diagonal element $H_{mm}(t)$ is the electronic transition energy between the local excited state $|m\rangle$ and the ground state, i.e., the site energy of the pigment m, while the off-diagonal element $H_{mn}(t)$ with m $\neq$ n is the excitonic coupling between states $|m\rangle$ and $\langle n|$. Furthermore, the protein environment is described by a set of harmonic oscillators obtained from a normal mode analysis where the Q_{ξ} and P_{ξ} are the dimensionless coordinates and momenta of the systems, respectively, which are expressed in terms of the creation and annihilation operators of vibrational quanta, $C_{\xi}^{\dagger}$ and C_{ξ}, respectively, of normal mode ξ as [60]:

$$Q_{\xi} = (C_{\xi}^{\dagger} + C_{\xi}) \quad \text{and} \quad Q_{\xi} = i(C_{\xi}^{\dagger} - C_{\xi}). \tag{21}$$

Alternatively, these dimensionless coordinates and momenta can also be expressed in terms of the mass-weighted normal coordinates q_ξ and momenta p_ξ as [60]:

$$Q_\xi = \sqrt{\frac{2\omega_\xi}{\hbar}} q_\xi \quad \text{and} \quad P_\xi = \sqrt{\frac{2}{\omega_\xi \hbar}} p_\xi. \tag{22}$$

The time dependence of $H_{mn}(t)$ for the light harvesting complex can be introduced from the nuclear dynamics caused by the coupling between the pigment and protein, which, following [60], can be expressed as the Taylor series expansion of the small displacements $R_j(t)$ of atoms from their equilibrium positions $R_j^{(0)}$ as:

$$H_{mn}(t) \approx H_{mn}^{(0)} + \sum_j (\nabla_j H_{mn}|_0) \cdot (R_j(t) - R_j^{(0)}), \tag{23}$$

where $H_{mn}^{(0)}$ and $\nabla_j H_{mn}|_0$ are the values of the Hamiltonian and its gradient taken w.r.t the three Cartesian coordinates of the jth atom, respectively, at the equilibrium position of nuclei in the electronic ground state. In addition, the displacement of the jth atom in terms of its weighted mass M_j can be expressed as [60,111]

$$R_j(t) - R_j^{(0)} = M_j^{-\frac{1}{2}} \sum_\xi A_j^{(\xi)} q_\xi(t), \tag{24}$$

where $A_j^{(\xi)}$ contains the contributions of the jth atom to the eigenvector of normal mode ξ. From the above equations, the total time-dependent Hamiltonian can be expressed as (see details, e.g., in [60,111])

$$H_{mn}(t) \approx H_{mn}^{(0)} + \sum_\xi \hbar \omega_\xi g_\xi(m,n) Q_\xi(t), \tag{25}$$

where $g_\xi(m,n)$ describes the coupling between the two sites and is given by

$$g_\xi(m,n) = \omega_\xi^{-\frac{3}{2}} (2\hbar)^{-\frac{1}{2}} \sum_j M_j^{-\frac{1}{2}} (\nabla_j H_{mn}|_0) A_j^{(\xi)}. \tag{26}$$

Furthermore, $g_\xi(m,n)$ is computed by using the Poisson–TrEsp method and details about the same can be found in [108,111,112]. Notably, using this coupling constant, we can calculate the spectral density as

$$J_{mnkl}(\omega) = \sum_\xi g_\xi(m,n) g_\xi(k,l) \delta(\omega - \omega_\xi). \tag{27}$$

The expression for the spectral density described in Equation (27) can be further used to calculate the fluctuation of the energy at a particular site during the excitonic dynamics of the FMO protein system. By varying the indices in Equation (27), one can easily calculate the coupling fluctuation including the correlations between the site energy fluctuations.

2.6. Time-Dependent Density Functional Theory

The properties like excitonic energy transfer and spectral density are time-dependent phenomena and their properties in light harvesting complexes can be computed utilizing the time-dependent density functional theory (TDDFT). Several studies have been reported in the literature for computing the energy transfer and excitonic energy within the biological complexes associated with the photosynthesis process utilizing the TDDFT [113–117]. More details about the application of DFT in long-range interaction, along with its use in the large molecular systems, can be found in [118–121]. The theory behind the applicability of TDDFT for large molecules is briefly highlighted below.

In order to describe the application of the TDDFT to explain the properties of the biomolecules like BChls present in the FMO complex in their respective states, we will follow the procedure given

in [118]. The time-dependent Kohn–Sham equation Equation (28) for an independent particle system can be derived assuming the existence of an effective potential v_{eff}, whose orbitals $\Psi(r,t)$ yield the same charge density as for the interacting system [118,122,123]

$$\left[-\frac{1}{2}\nabla^2 + v_{eff}(r,t)\right]\Psi(r,t) = -i\frac{\partial}{\partial t}\Psi(r,t). \tag{28}$$

The effective potential can be expressed as the sum of applied field (perturbation) ($v(t)$) and self-consistent field ($v_{SCF}(r,t)$):

$$v_{eff}(r,t) = v(t) + v_{SCF}(r,t). \tag{29}$$

Furthermore, the self-consistent field ($v_{SCF}(r,t)$) is expressed as:

$$v_{SCF}(r,t) = \int \frac{\rho(r,t)}{|r-r'|} + v_{xc}(r,t), \tag{30}$$

where the quantity $v_{xc}(r,t)$ is the exchange-correlation potential that can be expressed as the functional derivative of the exchange-correlation action A_{xc} as:

$$v_{xc}[\rho](r,t) = \frac{\delta A_{xc}[\rho]}{\delta\rho(r,t)} \approx \frac{\delta E_{xc}[\rho_t]}{\delta\rho_t(r)} = v_{xc}[\rho_t](r), \tag{31}$$

where the unknown functional (A_{xc}) of ρ over both time and space is approximated by the exchange-correlation functional (E_{xc}) of the time-independent Kohn–Sham theory which is a function of ρ_t of space at fixed t.

In most of the time-dependent phenomena involving excitations such as the photosynthesis process, the energy transfer is supposed to be perturbed by the incident light. Therefore, in the presence of small perturbations of the system, $\delta v(t)$ will give the following effective potential [118]:

$$\delta v_{eff}(r,t) = \delta v(t) + \delta v_{SCF}(r,t), \tag{32}$$

where $\delta v_{SCF}(r,t)$ is the linear response of the self-consistent field arising from the change in the charge density as given by (in frequency representation):

$$\delta\rho(r,\omega) = \sum_{ai}\delta P_{ai}(\omega)\Psi_a(r)\Psi_i^*(r) + \sum_{ia}\delta P_{ia}(\omega)\Psi_i(r)\Psi_a^*(r), \tag{33}$$

where $\delta P_{st}(\omega)$ is the linear response of the Kohn–Sham density matrix in the basis of the unperturbed molecular orbitals (i, j for occupied; a, b for virtual; s, t, u, v for general orbitals). Furthermore, the linear response of the Kohn–Sham density matrix to the applied field utilizing the elementary results from time-dependent perturbation theory can be expressed as:

$$\delta P_{st}(\omega) = \frac{\Delta n_{st}}{(\epsilon_s - \epsilon_t) - \omega}\delta v_{st}^{eff}(\omega), \tag{34}$$

where Δn_{st} is the difference in occupation numbers, $\Delta n_{st} = 1$ for $st = ai$ and $\Delta n_{st} = -1$ for $st = ia$. Furthermore, the potential δv_{SCF} depends on the density matrix response as [118]:

$$\delta v_{st}^{SCF}(\omega) = \sum_{uv} K_{st,uv}(\omega)\delta P_{uv}(\omega) = \sum_{bj} K_{st,bj}(\omega)\delta P_{bj}(\omega) + \sum_{jb} K_{st,jb}(\omega)\delta P_{jb}(\omega), \tag{35}$$

where K is the coupling matrix for TDDFT which can be expressed as

$$K_{st\sigma,uv\tau} = \frac{\partial v_{st}^{SCF}}{\partial P_{uv}} = \frac{\partial v_{st}^{Coul}}{\partial P_{uv}} + \frac{\partial v_{st}^{xc}}{\partial P_{uv}} = \langle \Psi_{s\sigma}^*(r)\Psi_{t\sigma}(r)|\Psi_{u\tau}^*(r')\Psi_{v\tau}(r')\rangle + \int drdr'\Psi_{s\sigma}^*(r)\Psi_{t\sigma}(r)\frac{\delta^2 E_{xc}}{\delta\rho_\sigma(r)\delta\rho_\tau(r')}\Psi_{v\tau}^*(r')\Psi_{u\tau}(r'). \quad (36)$$

In the TDDFT calculations, the quantity describing the emission or absorption transition probability between the two different energy levels of molecular systems is defined by the oscillator strength. In photosynthesis, this is also a very important parameter. Assuming that Ψ_0 and Ψ_I are the wave functions for the ground state and excited state of the molecular system, respectively, the oscillator strength of this transition can be expressed as [122]

$$f_I = \frac{2}{3}(E_I - E_0)\sum_{k=x,y,z}\langle\Psi_0|r_k|\Psi_I\rangle, \quad (37)$$

where E_0 and E_I are the energies of the ground and excited states of the system between which the transition is taking place.

3. Energetic and Spectroscopic Properties Using DFT

In this section, we highlight some of the insightful calculations performed on the BChls from the FMO complexes. Specifically, we describe the results for the NMR properties of the BChls taken from the FMO complex as described in our group's recent work in [124–126]. In this study, the NMR magnetic shielding tensors were calculated using the DFT implemented by the Gaussian 09 set of programs [127], in particular, the NMR spectra were computed using the density functional PBE1PBE developed by Purdue, Burke and Ernzerhof [128–130]. The gauge-including atomic orbital (GIAO) method was used for the calculation of the NMR properties. The chemical shift was calculated by taking the difference in the shielding tensors of carbon atom in BChl from the shielding tensor of the carbon atom in TMS. The Gaussian broadening was added to the NMR spectra for the chemical shifts of the carbon atoms. The structures of the FMO complex used in this study were taken from the protein data bank [17,18] and the structure of chlorophyll *a* was taken from [27]. Furthermore, the separation of different chlorophylls was achieved by using VMD, a molecular visualization software [131]. The HOMO and LUMO energies, and the energy gap for individual BChls from the FMO complex were computed using the TDDFT implemented by the Gaussian 09 program. Table 1 presents the computed HOMO and LUMO energies, along with the HOMO-LUMO gap that characterizes the excitation properties of the molecular system. The Avogadro software was used for post-processing of the Gaussian output. Three-dimensional structures emphasizing the HOMO and LUMO in the BChl system taken from the FMO complex have been calculated by using DFT and presented in Figure 6. Here, the TDDFT was also used to calculate the first six excited states of two different BChls along with the oscillator strength of each excited state. The results for the energy and oscillator strength of the BChl systems are given in Table 2.

The quantity oscillator strength calculated for the BChl pigments in the FMO complex describe the chances of the energy exchange via emission or absorption of the electromagnetic energy during the light harvesting for the process of photosynthesis. The values of the oscillator strengths calculated for two different BChls corresponding to various set transitions are distinct. In addition, the transition energy to the ground state from the higher level is increasing with the increase in the energy levels. The multiple excited states observed in the FMO complex are also due to the presence of different BChls in different local environments of the protein. While still debated, the possibility of existence of the long-lived quantum coherence also motivates to intensify the computational studies in different directions including the study of the excitation properties using different types of computational techniques [4,11,13,20,71,94,132–142].

Table 1. HOMO and LUMO energies for the different types of BChls taken from the FMO light harvesting complex.

Type	HOMO (eV)	LUMO (eV)	Gap
BChl 1	−5.286	−3.202	2.084
BChl 2	−4.669	−3.1	1.569
BChl 3	−4.394	−2.1	2.294
BChl 4	−5.142	−3.102	2.04
BChl 5	−5.499	−4.361	1.138
BChl 6	−5.247	−3.091	2.156
BChl 7	−5.331	−3.245	2.086

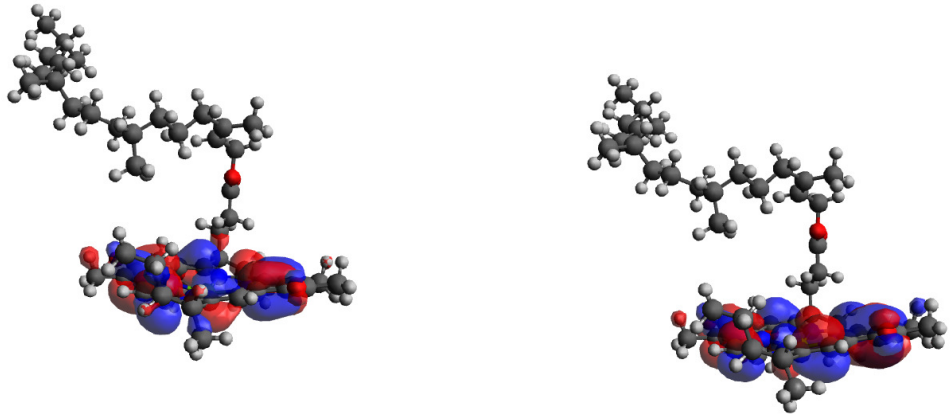

Figure 6. (Color online) (**a**) HOMO and (**b**) LUMO representation for one of the BChls using TDDFT.

Table 2. Calculation of the excitation energy, wavelength and oscillator strength of the first six excited states for two different BChls calculated by using time-dependent density functional theory.

Excitation	BChl 6			BChl 7		
	Energy (eV)	Wavelength (nm)	f	Energy (eV)	Wavelength (nm)	f
S0-S1	1.9035	651.35	0.3489	0.7744	1601.08	0.0025
S0-S2	2.2434	552.67	0.1275	1.0929	1134.41	0.0078
S0-S3	2.9733	416.99	0.0007	1.1909	1041.14	0.0172
S0-S4	3.0891	401.36	0.000	1.7776	697.48	0.148
S0-S5	3.1408	394.75	0.0026	1.9835	625.07	0.0146
S0-S6	3.3296	372.37	0.0066	2.1139	586.51	0.357

4. Applications of Photosynthetic Systems

Photosynthesis and the associated light harvesting complexes have a range of important applications in biomedicine, environment and energy harvesting. In this section, we will discuss about some of the current and potential applications of photosynthetic systems.

4.1. Environmental Science Applications

Over the past years, significant research efforts have been devoted for the production of energy from biomass to meet the increasing energy demands worldwide and keeping a check on the environmental issues. Microorganisms such as cyanobacteria and microalgae possess a significant potential in the production of biofuels, chemicals, and bio-based products for meeting the global energy crisis [143–150]. Such renewable alternatives would not only limit the reliance on fossil fuel resources

but could also serve as a stepping stone for effective transition from a petroleum-based economy to a bio-based economy [145,148]. Notably, the microbial fuel cell represents a promising alternative of electricity generation from the catalysis of microorganisms found in lakes, lagoons, ponds, or even waste water reserves [151–153]. Microalgae is one of the examples of the photosynthetic bioorganisms that is used for the production of green bioelectricity utilizing microbial fuel cells. Furthermore, owing to the natural abundance of such living microorganisms, the bioelectricity produced is a highly cost-effective and sustainable alternative for meeting the energy demands of the growing population. However, the large-scale industrial translation of this technology is currently limited owing to several biotechnological, economic and environmental issues. Some of the associated bottlenecks, mainly related to its low stability and efficiency, can be effectively tackled by the synergetic combination of synthetic biology and nanotechnology. For example, the native electrogenic capacity and the working lifetimes of microbiological cells can be augmented utilizing the tunability of nanomaterials. More recently, an overview of the different nanomaterials used to enhance bioelectricity generation through improved photosynthesis, extracellular electron transfer and anode performance have been reviewed in [153]. More details about the photosynthetic microbial fuel cells and their integration with the conventional technology of the microbial fuel cell can be found in [154–159]. The photosynthesis can also be used for energy storage, as described in [160–165].

The effects of different kinds of light sources on the production of biomass and pigments have been studied in the photosynthetic bacteria waste water treatment in [166]. The applications, opportunities and challenges of using microalgae group Chlorophyta for various energy and environmental applications have been reviewed in [167], highlighting some critical aspects such as the applicability of Chlorophyta in industrial and domestic waste water treatment, and removal of contaminating nutrients. Recent research advances in the waste water treatment utilizing the freshwater monocultures of filamentous algae have been reviewed and critically analyzed in [168], mainly focusing on microalgae and polyculture systems. Research gaps in translating this technology to large-scale system design, including species selection criteria, the effect of nutrient type and loading conditions, inorganic carbon supply, algae–bacteria interactions and parameters, viz., pond depth, mixing and harvesting regimes were identified along with providing a future road map for maximizing productivity and waste water treatment efficiency [168]. Furthermore, the green algae (Chlorella Kessleri) is one of the most common light harvesting complexes found in the water which can be used to measure the purity of water utilizing rigorous study of photosynthesis phenomena in them. This can be done by measuring the concentration of oxygen produced by photosynthesis in water containing green algae [169–171].

The detailed understanding and analysis of quantum coherence and spectral density in the light harvesting complexes would also be helpful in the understanding of processes pertinent to the solar and photovoltaic cells [172–178]. Recently, different theoretical models used for describing energy absorption and transmission in solar cells and photosynthetic systems, including the FMO complex, have been critically analyzed in [179]. This study highlights that the use of sinks, traps or any artificial relaxation process in the standard theoretical models of solar energy conversion, which is developed for studying the energy transfer to the reaction center in photosynthetic systems may contradict to the second law of thermodynamics. These findings could invalidate several existing models used for studying solar energy conversion and raise significant concerns regarding some of the earlier drawn conclusions. A possible solution to address this issue has been put forward in [179] by providing a thermodynamically-consistent version of the model that explicitly describes parts of the reaction center and employs a Hamiltonian transfer to describe the energy absorption and transmission instead of a decay rate or sink term. Owing to the difficulties to probe molecular self-assembling and packing structures at the atomic level by experimental techniques, theoretical simulations are becoming a useful tool in our better understanding of the structure–property relationship of the electronic processes for organic solar cells [180–185]. Recent advances in the theoretical simulations for organic solar cells ranging from the molecular dynamics simulated packing structures to the electronic processes computed by quantum-chemical, in combination with kinetic Monte Carlo, simulations have been

reviewed in [180]. The future perspective and challenges associated with the prediction of electrical characteristics and photoelectric conversion efficiencies of organic solar cells from molecular structures utilizing theoretical simulations have also been highlighted in [180].

4.2. Biomimetic Applications

Artificial photosynthesis is envisioned as a promising technique for harvesting solar energy through water splitting and CO_2 reduction to generate high-energy chemical fuels [144,186–190]. Although the field of artificial photosynthesis is still in its infancy phase of research, recent advances in synthetic biology have provided a significant boost to this interdisciplinary research field. The main goal of artificial photosynthesis is to assemble molecular systems into larger-scale constructs for replicating the natural processes of photosynthesis which is a quite challenging and complex task in itself [190]. Today, artificial photosynthesis is largely focused on understanding and mimicking the ultimate functionality of the natural photosynthetic phenomena for producing energy-rich fuel using cheap and environmentally friendly biomimetic compounds [188,190]. Thus, the essential components of an artificial photosynthetic device would be: (i) a light harvester (e.g., semiconductor) for converting solar photons to excited states, generation of charge-separation and regulation of the flow of collected excitation energy to the reaction sites, (ii) a reduction active reaction site and an oxidation active reaction site, where conversion of excited states to redox potential occurs, (iii) molecular catalysts (i.e., transition metal complexes) to assist water splitting and CO_2 reduction system, and (iv) linkages of different molecular and nano- and macro-scale components of artificial photosynthetic elements [144,188,189,191].

The artificial photosynthesis is a good source of production of chemical energy that can be used to reduce the amount of carbon dioxide present in the environment [192–202]. The use of artificial fertilizers has been increased in the past few decades for boosting food productivity for satisfying the needs of the growing population [203,204]. The increased consumption also brings production of the byproducts of the natural processes occurring on a daily basis that can be utilized in the production of sustainable and green energy utilizing artificial photosynthesis. Several computational techniques are also available in the literature for studying artificial photosynthesis [205–208]. In addition, the use of the small molecules to trigger the photosynthesis reaction has been recently studied in [209–214].

4.3. Health and Applications in Medicine

An exciting application of nano-sized self-assemblies of the chlorosomes found in the green sulfur as a contrast agent for medical imaging for visualizing different structures and pathologies within the human body has been demonstrated in [215–218]. The feasibility and potential of such studies can be attributed to the fact that light harvesting antennas like chlorosomes have a special structure through which they can absorb light even from the region with very low intensity of light source. The previtamin D3 from 7-dehydrochlorostel level can also be determined in human skin by studying photosynthesis in them through exposure to sunlight [219,220]. The photosynthetic bacteria are also a good source of vitamin B12 and have been used in some of the important medical applications, including the treatment of anemia, neuritis and eye problems [124]. Other applications of photosynthetic bacteria include the production of coenzyme Q10 that is used for treating heart disease, brain vascular injury and anemia [124]. These bacteria can also be used to produce the porphyrin and ribonucleic acids (RNA) that again can potentially be used in treating several diseases and deficiencies in the human body [124].

4.4. Enhancing the Quantum Efficiency of Excitonic Energy Transfer and Ultrafast Processes in Light Harvesting Complexes

Valuable lessons can be learned from the operating principle of photosynthesis that is a highly optimized process whose primary steps involve transport of energy while operating near theoretical quantum limits of efficiency [69,221]. In recent years, there have been significant research efforts that

have been motivated by the hypothesis that nature may use quantum coherences to direct energy transfer [69,221]. There has been a resurgence of interest in quantum biology owing to the advances in experimental and computational techniques to accurately capture the quantum phenomena in biological systems at smaller length and timescales [144,222]. Notably, quantum effects in biology have been extensively studied in the FMO complex and small photosynthetic light harvesting antennas of bacteria and plants. Apart from our better understanding of quantum effects in these biological systems, these studies also pave the way for the rational design of optimal molecular photonic structures to achieve efficient transport of excitons [144,223]. Such analysis would be quite useful in designing organic semiconductors that provide an attractive alternative for the sustainable production of materials and devices in some of the emerging applications, such as consumer electronics, solar energy capture, photocatalysis, quantum computing, communication and sensing [223,224]. Clearly, a lot of work has to be done in this direction to test the proposed hypothesis, address raised controversies and discover many more functional quantum behavior [69,221]. Recall, e.g., earlier reported results claiming that the dynamic long-lived electronic quantum coherence in the FMO BChl complex explain its extreme efficiency that allows them to sample vast areas of phase space for finding the most efficient path [139]. However, more recent evidence indicates that the observed long-lived coherences originate from impulsively excited vibrations and are too fast for electronic coherences to play a significant role in the exciton transfer between pigments [69,225]. Even more recently, the effect of underdamped intramolecular vibrational modes on enhancing excitation energy transfer has been investigated in [226], using the approach based on the numerically exact hierarchy equation of motion. This study reported that the weakly coupled underdamped vibrational mode fuels a faster excitation energy transfer, elucidating that long-lived vibrations can, in principle, enhance energy transfer, without involving long-lived electronic coherence [226]. Thus, more studies are needed in this intrinsically interdisciplinary research field, not only to improve our understanding of the mechanisms behind the fundamental photosynthetic process of nature, but also to transfer these ideas into the next-generation artificial light-harvesting materials.

5. Conclusions

The purpose of this review has been to shed better light on the computational and mathematical techniques used for studying the photosynthetic systems and phenomena of light harvesting complexes, with special attention given to the FMO complex of green bacteria. Among other issues, we have focused on spectral density, quantum coherence, and coupling between exciton and phonon dynamics of the FMO complexes. The application of the TDDFT has also been discussed as an essential tool for computing the excitation energy of biological complexes associated with the photosynthetic systems. Therefore, we have also highlighted and systematically analyzed some of the recent results on the excitation energy and corresponding oscillator strength of different BChls present in the FMO light harvesting complexes. Finally, the potential and emerging applications of the photosynthetic systems associated with light harvesting complexes have been presented in the fields of environmental sciences, energy, health, and sustainable development.

Author Contributions: Conceptualization, R.M.; methodology, S.B. and S.S.; software, S.B.; writing—original draft preparation, S.B. and S.S.; writing—review and editing, R.M., S.B., and S.S.; supervision, R.M. All authors have read and agreed to the published version of the manuscript.

Funding: This research was funded by the Natural Sciences and Engineering Research Council (NSERC) of Canada and Canada Research Chairs (CRC) Program.

Acknowledgments: This work was made possible by the facilities of the Shared Hierarchical Academic Research Computing Network (SHARCNET:www.sharcnet.ca) and Compute/Calcul Canada. The authors are grateful to P. J. Douglas Roberts for helping with technical SHARCNET computational aspects. R.M. is also acknowledging the support of the BERC 2018–2021 program and Spanish Ministry of Science, Innovation and Universities through the Agencia Estatal de Investigacion (AEI) BCAM Severo Ochoa excellence accreditation SEV-2017-0718, and the Basque Government fund AI in BCAM EXP. 2019/00432.

Conflicts of Interest: The authors declare no conflict of interest.

References

1. Wen, J.; Tsukatani, Y.; Cui, W.; Zhang, H.; Gross, M.L.; Bryant, D.A.; Blankenship, R.E. Structural model and spectroscopic characteristics of the FMO antenna protein from the aerobic chlorophototroph, Candidatus Chloracidobacterium thermophilum. *Biochim. Biophys. Acta (BBA)-Bioenerg.* **2011**, *1807*, 157–164. [CrossRef] [PubMed]
2. Baker, L.A.; Habershon, S. Photosynthetic pigment-protein complexes as highly connected networks: Implications for robust energy transport. *Proc. R. Soc. A Math. Phys. Eng. Sci.* **2017**, *473*, 20170112. [CrossRef] [PubMed]
3. Wen, J.; Zhang, H.; Gross, M.L.; Blankenship, R.E. Membrane orientation of the FMO antenna protein from Chlorobaculum tepidum as determined by mass spectrometry-based footprinting. *Proc. Natl. Acad. Sci. USA* **2009**, *106*, 6134–6139. [CrossRef]
4. Leng, X.; Yan, Y.M.; Zhu, R.D.; Song, K.; Weng, Y.X.; Shi, Q. Simulation of the two-dimensional electronic spectroscopy and energy transfer dynamics of light-harvesting complex ii at ambient temperature. *J. Phys. Chem. B* **2018**, *122*, 4642–4652. [CrossRef]
5. Nielsen, A.Z.; Ziersen, B.; Jensen, K.; Lassen, L.M.; Olsen, C.E.; Møller, B.L.; Jensen, P.E. Redirecting Photosynthetic Reducing Power toward Bioactive Natural Product Synthesis. *ACS Synth. Biol.* **2013**, *2*, 308–315. [CrossRef]
6. Sasaki, K.; Watanabe, M.; Suda, Y.; Ishizuka, A.; Noparatnaraporn, N. Applications of photosynthetic bacteria for medical fields. *J. Biosci. Bioeng.* **2005**, *100*, 481–488. [CrossRef]
7. Suchkov, S.; Herrera, A.S. The role of human photosynthesis in predictive, preventive and personalized medicine. *EPMA J* **2014**, *5*, A146. [CrossRef]
8. Wang, H.; Zhang, G.; Peng, M.; Zhou, Q.; Li, J.; Xu, H.; Meng, F. Synthetic white spirit wastewater treatment and biomass recovery by photosynthetic bacteria: Feasibility and process influence factors. *Int. Biodeterior. Biodegrad.* **2016**, *113*, 134–138. [CrossRef]
9. Hohmann-Marriott, M.F.; Blankenship, R.E. Variable fluorescence in green sulfur bacteria. *Biochim. Biophys. Acta (BBA)-Bioenerg.* **2007**, *1767*, 106–113. [CrossRef]
10. Bína, D.; Gardian, Z.; Vácha, F.; Litvín, R. Native FMO-reaction center supercomplex in green sulfur bacteria: An electron microscopy study. *Photosynth. Res.* **2016**, *128*, 93–102. [CrossRef]
11. Kramer, T.; Rodriguez, M. Two-dimensional electronic spectra of the photosynthetic apparatus of green sulfur bacteria. *Sci. Rep.* **2017**, *7*, 45245. [CrossRef]
12. Karafyllidis, I.G. Quantum transport in the FMO photosynthetic light-harvesting complex. *J. Biol. Phys.* **2017**, *43*, 239–245. [CrossRef]
13. Kramer, T.; Noack, M.; Reinefeld, A.; Rodríguez, M.; Zelinskyy, Y. Efficient calculation of open quantum system dynamics and time-resolved spectroscopy with distributed memory HEOM (DM-HEOM). *J. Comput. Chem.* **2018**, *39*, 1779–1794. [CrossRef]
14. Rathbone, H.W.; Davis, J.A.; Michie, K.A.; Goodchild, S.C.; Robertson, N.O.; Curmi, P.M. Coherent phenomena in photosynthetic light harvesting: Part one—Theory and spectroscopy. *Biophys. Rev.* **2018**, *10*, 1427–1441. [CrossRef]
15. Rathbone, H.W.; Davis, J.A.; Michie, K.A.; Goodchild, S.C.; Robertson, N.O.; Curmi, P.M. Coherent phenomena in photosynthetic light harvesting: Part two—Observations in biological systems. *Biophys. Rev.* **2018**, *10*, 1443–1463. [CrossRef]
16. Saer, R.G.; Schultz, R.L.; Blankenship, R.E. The influence of quaternary structure on the stability of Fenna–Matthews–Olson (FMO) antenna complexes. *Photosynth. Res.* **2019**, *140*, 39–49. [CrossRef]
17. Tronrud, D.E.; Wen, J.; Gay, L.; Blankenship, R.E. The structural basis for the difference in absorbance spectra for the FMO antenna protein from various green sulfur bacteria. *Photosynth. Res.* **2009**, *100*, 79–87. [CrossRef]
18. Wen, J.; Zhang, H.; Gross, M.L.; Blankenship, R.E. Native Electrospray Mass Spectrometry Reveals the Nature and Stoichiometry of Pigments in the FMO Photosynthetic Antenna Protein. *Biochemistry* **2011**, *50*, 3502–3511. [CrossRef]
19. Cui, X.; Yan, Y.; Wei, J. Theoretical Study on the Effect of Environment on Excitation Energy Transfer in Photosynthetic Light-Harvesting Systems. *J. Phys. Chem. B* **2020**, *124*, 2354–2362. [CrossRef]

20. Kim, Y.; Morozov, D.; Stadnytskyi, V.; Savikhin, S.; Slipchenko, L.V. Predictive First-Principles Modeling of a Photosynthetic Antenna Protein: The Fenna–Matthews–Olson Complex. *J. Phys. Chem. Lett.* **2020**, *11*, 1636–1643. [CrossRef]
21. Friemann, R.; Lee, K.; Brown, E.N.; Gibson, D.T.; Eklund, H.; Ramaswamy, S. Structures of the multicomponent Rieske non-heme iron toluene 2,3-dioxygenase enzyme system. *Acta Crystallogr. Sect. D* **2009**, *65*, 24–33. [CrossRef] [PubMed]
22. Camara-Artigas, A.; Blankenship, R.E.; Allen, J.P. The structure of the FMO protein from Chlorobium tepidum at 2.2 Ã resolution. *Photosynth. Res.* **2003**, *75*, 49–55. [CrossRef]
23. Jia, X.; Mei, Y.; Zhang, J.Z.H.; Mo, Y. Hybrid QM/MM study of FMO complex with polarized protein-specific charge. *Sci. Rep.* **2015**, *5*, 17096. [CrossRef]
24. Gammeren, A.J.V.; Hulsbergen, F.B.; Erkelens, C.; Groot, H.J.M.D. Synthetic analogues of the histidine–chlorophyll complex: A NMR study to mimic structural features of the photosynthetic reaction center and the light-harvesting complex. *J. Biol. Inorg. Chem.* **2004**, *9*, 109–117. [CrossRef]
25. Makarska-Bialokoz, M.; Kaczor, A.A. Computational Analysis of Chlorophyll Structure and UV-Vis Spectra: A Student Research Project on the Spectroscopy of Natural Complexes. *Spectrosc. Lett.* **2014**, *47*, 147–152. [CrossRef]
26. Sinnecker, S.; Koch, W.; Lubitz, W. Chlorophyll a Radical Ions: A Density Functional Study. *J. Phys. Chem. B* **2002**, *106*, 5281–5288. [CrossRef]
27. Sundholm, D. Density functional theory calculations of the visible spectrum of chlorophyll a. *Chem. Phys. Lett.* **1999**, *302*, 480–484. [CrossRef]
28. Taguchi, A.T.; O'Malley, P.J.; Wraight, C.A.; Dikanov, S.A. Nuclear Hyperfine and Quadrupole Tensor Characterization of the Nitrogen Hydrogen Bond Donors to the Semiquinone of the QB Site in Bacterial Reaction Centers: A Combined X- and S-Band 14,15N ESEEM and DFT Study. *J. Phys. Chem. B* **2014**, *118*, 1501–1509. [CrossRef]
29. Xu, J.; Terskikh, V.V.; Huang, Y. 25Mg Solid-State NMR: A Sensitive Probe of Adsorbing Guest Molecules on a Metal Center in Metal-Organic Framework CPO-27-Mg. *J. Phys. Chem. Lett.* **2013**, *4*, 7–11. [CrossRef]
30. Kacprzak, S.; Kaupp, M. Electronic g-Tensors of Semiquinones in Photosynthetic Reaction Centers. A Density Functional Study. *J. Phys. Chem. B* **2004**, *108*, 2464–2469. [CrossRef]
31. Lumpkin, O. 25Mg and 14N nuclear quadrupole resonances in chlorophyll-a and magnesium phthalocyanine. *J. Chem. Phys.* **1975**, *62*, 3281–3283. [CrossRef]
32. Hoyer, S.; Sarovar, M.; Whaley, K.B. Limits of quantum speedup in photosynthetic light harvesting. *New J. Phys.* **2010**, *12*, 065041. [CrossRef]
33. Ishizaki, A.; Fleming, G.R. On the Interpretation of Quantum Coherent Beats Observed in Two-Dimensional Electronic Spectra of Photosynthetic Light Harvesting Complexes. *J. Phys. Chem. B* **2011**, *115*, 6227–6233. [CrossRef]
34. Scholes, G.D. Quantum-Coherent Electronic Energy Transfer: Did Nature Think of It First? *J. Phys. Chem. Lett.* **2010**, *1*, 2–8. [CrossRef]
35. Shim, S.; Rebentrost, P.; Valleau, S.; Aspuru-Guzik, A. Atomistic Study of the Long-Lived Quantum Coherences in the Fenna–Matthews–Olson Complex. *Biophys. J.* **2012**, *102*, 649–660. [CrossRef]
36. Ghosh, S.; Bishop, M.M.; Roscioli, J.D.; LaFountain, A.M.; Frank, H.A.; Beck, W.F. Excitation Energy Transfer by Coherent and Incoherent Mechanisms in the Peridinin-Chlorophyll a Protein. *J. Phys. Chem. Lett.* **2017**, *8*, 463–469. [CrossRef]
37. Rafiq, S.; Scholes, G.D. From Fundamental Theories to Quantum Coherences in Electron Transfer. *J. Am. Chem. Soc.* **2018**, *141*, 708–722. [CrossRef]
38. Thyrhaug, E.; Tempelaar, R.; Alcocer, M.J.; Žídek, K.; Bína, D.; Knoester, J.; Jansen, T.L.; Zigmantas, D. Identification and characterization of diverse coherences in the Fenna–Matthews–Olson complex. *Nat. Chem.* **2018**, *10*, 780. [CrossRef]
39. Irgen-Gioro, S.; Spencer, A.P.; Hutson, W.O.; Harel, E. Coherences of bacteriochlorophyll a uncovered using 3D-electronic spectroscopy. *J. Phys. Chem. Lett.* **2018**, *9*, 6077–6081. [CrossRef]
40. Maiuri, M.; Ostroumov, E.E.; Saer, R.G.; Blankenship, R.E.; Scholes, G.D. Coherent wavepackets in the Fenna–Matthews–Olson complex are robust to excitonic-structure perturbations caused by mutagenesis. *Nat. Chem.* **2018**, *10*, 177. [CrossRef]

41. Jumper, C.C.; Rafiq, S.; Wang, S.; Scholes, G.D. From coherent to vibronic light harvesting in photosynthesis. *Curr. Opin. Chem. Biol.* **2018**, *47*, 39–46. [CrossRef]
42. Meneghin, E.; Pedron, D.; Collini, E. Characterization of the coherent dynamics of bacteriochlorophyll a in solution. *Chem. Phys.* **2019**, *519*, 85–91. [CrossRef]
43. Vassiliev, I.R.; Kjær, B.; Schorner, G.L.; Scheller, H.V.; Golbeck, J.H. Photoinduced Transient Absorbance Spectra of P840/P840+ and the FMO Protein in Reaction Centers of Chlorobium vibrioforme. *Biophys. J.* **2001**, *81*, 382–393. [CrossRef]
44. Saer, R.G.; Stadnytskyi, V.; Magdaong, N.C.; Goodson, C.; Savikhin, S.; Blankenship, R.E. Probing the excitonic landscape of the Chlorobaculum tepidum Fenna-Matthews-Olson (FMO) complex: A mutagenesis approach. *Biochim. Biophys. Acta (BBA)-Bioenerg.* **2017**, *1858*, 288–296. [CrossRef]
45. Saer, R.; Orf, G.S.; Lu, X.; Zhang, H.; Cuneo, M.J.; Myles, D.A.A.; Blankenship, R.E. Perturbation of bacteriochlorophyll molecules in Fenna–Matthews–Olson protein complexes through mutagenesis of cysteine residues. *Biochim. Biophys. Acta (BBA)-Bioenerg.* **2016**, *1857*, 1455–1463. [CrossRef]
46. Rolczynski, B.S.; Navotnaya, P.; Sussman, H.R.; Engel, G.S. Cysteine-mediated mechanism disrupts energy transfer to prevent photooxidation. *Proc. Natl. Acad. Sci. USA* **2016**, *113*, 8562–8564. [CrossRef]
47. Orf, G.S.; Saer, R.G.; Niedzwiedzki, D.M.; Zhang, H.; McIntosh, C.L.; Schultz, J.W.; Mirica, L.M.; Blankenship, R.E. Evidence for a cysteine-mediated mechanism of excitation energy regulation in a photosynthetic antenna complex. *Proc. Natl. Acad. Sci. USA* **2016**, *113*, E4486–E4493. [CrossRef]
48. Li, Y.; Cai, Z.L.; Chen, M. Spectroscopic Properties of Chlorophyll f. *J. Phys. Chem. B* **2013**, *117*, 11309–11317. [CrossRef]
49. O'Malley, P.J.; Collins, S.J. The Effect of Axial Mg Ligation on the Geometry and Spin Density Distribution of Chlorophyll and Bacteriochlorophyll Cation Free Radical Models: A Density Functional Study. *J. Am. Chem. Soc.* **2001**, *123*, 11042–11046. [CrossRef]
50. Adolphs, J.; Renger, T. How Proteins Trigger Excitation Energy Transfer in the FMO Complex of Green Sulfur Bacteria. *Biophys. J.* **2006**, *91*, 2778–2797. [CrossRef]
51. Kramer, T.; Kreisbeck, C. Modelling excitonic-energy transfer in light-harvesting complexes. In *AIP Conference Proceedings*; American Institute of Physics: College Park, MD, USA, 2014; Volume 1575, pp. 111–135.
52. Kreisbeck, C.; Kramer, T. Long-Lived Electronic Coherence in Dissipative Exciton Dynamics of Light-Harvesting Complexes. *J. Phys. Chem. Lett.* **2012**, *3*, 2828–2833. [CrossRef]
53. Kreisbeck, C.; Kramer, T.; Rodríguez, M.; Hein, B. High-performance solution of hierarchical equations of motion for studying energy transfer in light-harvesting complexes. *J. Chem. Theory Comput.* **2011**, *7*, 2166–2174. [CrossRef] [PubMed]
54. Songi, L.; Shia, Q. Calculation of correlated initial state in the hierarchical equations of motion method using an imaginary time path integral approach. *J. Chem. Phys.* **2015**, *143*, 194106. [CrossRef] [PubMed]
55. Kim, C.W.; Rhee, Y.M. Constructing an Interpolated Potential Energy Surface of a Large Molecule: A Case Study with Bacteriochlorophyll a Model in the Fenna–Matthews–Olson Complex. *J. Chem. Theory Comput.* **2016**, *12*, 5235–5246. [CrossRef]
56. Albaugh, A.; Boateng, H.A.; Bradshaw, R.T.; Demerdash, O.N.; Dziedzic, J.; Mao, Y.; Margul, D.T.; Swails, J.; Zeng, Q.; Case, D.A.; et al. Advanced Potential Energy Surfaces for Molecular Simulation. *J. Phys. Chem. B* **2016**, *120*, 9811–9832. [CrossRef]
57. Lee, M.K.; Huo, P.; Coker, D.F. Semiclassical Path Integral Dynamics: Photosynthetic Energy Transfer with Realistic Environment Interactions. *Annu. Rev. Phys. Chem.* **2016**, *67*, 639–668. [CrossRef]
58. Lee, M.H.; Troisi, A. Vibronic enhancement of excitation energy transport: Interplay between local and non-local exciton-phonon interactions. *J. Chem. Phys.* **2017**, *146*, 075101. [CrossRef]
59. Varsano, D.; Caprasecca, S.; Coccia, E. Theoretical description of protein field effects on electronic excitations of biological chromophores. *J. Phys. Condens. Matter* **2017**, *29*, 013002. [CrossRef]
60. Renger, T.; Klinger, A.; Steinecker, F.; Schmidt Busch, M.; Numata, J.; Müh, F. Normal mode analysis of the spectral density of the Fenna–Matthews–Olson light-harvesting protein: How the protein dissipates the excess energy of excitons. *J. Phys. Chem. B* **2012**, *116*, 14565–14580. [CrossRef]
61. Liguori, N.; Croce, R.; Marrink, S.J.; Thallmair, S. Molecular dynamics simulations in photosynthesis. *Photosynth. Res.* **2020**, *144*, 273–295. [CrossRef]

62. Higashi, M.; Saito, S. Quantitative Evaluation of Site Energies and Their Fluctuations of Pigments in the Fenna–Matthews–Olson Complex with an Efficient Method for Generating a Potential Energy Surface. *J. Chem. Theory Comput.* **2016**, *12*, 4128–4137. [CrossRef] [PubMed]
63. Jurinovich, S.; Curutchet, C.; Mennucci, B. The Fenna–Matthews–Olson Protein Revisited: A Fully Polarizable (TD)DFT/MM Description. *ChemPhysChem* **2014**, *15*, 3194–3204. [CrossRef] [PubMed]
64. König, C.; Neugebauer, J. Protein Effects on the Optical Spectrum of the Fenna–Matthews–Olson Complex from Fully Quantum Chemical Calculations. *J. Chem. Theory Comput.* **2013**, *9*, 1808–1820. [CrossRef]
65. Thyrhaug, E.; Žídek, K.; Dostál, J.; Bína, D.; Zigmantas, D. Exciton Structure and Energy Transfer in the Fenna–Matthews–Olson Complex. *J. Phys. Chem. Lett.* **2016**, *7*, 1653–1660. [CrossRef] [PubMed]
66. Smyth, C. Measuring Quantum Effects in Photosynthetic Light-Harvesting Complexes with Multipartite Entanglement. Ph.D. Thesis, University of Toronto (Canada), Toronto, ON, Canada, 2015.
67. Aghtar, M.; Strümpfer, J.; Olbrich, C.; Schulten, K.; Kleinekathöfer, U. Different Types of Vibrations Interacting with Electronic Excitations in Phycoerythrin 545 and Fenna–Matthews–Olson Antenna Systems. *J. Phys. Chem. Lett.* **2014**, *5*, 3131–3137. [CrossRef] [PubMed]
68. Goez, A.; Jacob, C.R.; Neugebauer, J. Modeling environment effects on pigment site energies: Frozen density embedding with fully quantum-chemical protein densities. *Comput. Theor. Chem.* **2014**, *1040*, 347–359. [CrossRef]
69. Cao, J.; Cogdell, R.J.; Coker, D.F.; Duan, H.G.; Hauer, J.; Kleinekathöfer, U.; Jansen, T.L.; Mančal, T.; Miller, R.D.; Ogilvie, J.P.; et al. Quantum biology revisited. *Sci. Adv.* **2020**, *6*, eaaz4888. [CrossRef]
70. Wang, L.; Allodi, M.A.; Engel, G.S. Quantum coherences reveal excited-state dynamics in biophysical systems. *Nat. Rev. Chem.* **2019**, *3*, 477–490. [CrossRef]
71. Marcus, M.; Knee, G.C.; Datta, A. Towards a spectroscopic protocol for unambiguous detection of quantum coherence in excitonic energy transport. *Faraday Discuss.* **2019**, *221*, 110–132. [CrossRef]
72. Alvertis, A.M.; Barford, W.; Worster, S.B.; Burghardt, I.; Datta, A.; Dijkstra, A.; Fay, T.; Ghosh, S.; Grünbaum, T.; Habershon, S.; et al. Quantum coherence in complex environments: General discussion. *Faraday Discuss.* **2019**, *221*, 168–201. [CrossRef]
73. Mančal, T. A Decade with Quantum Coherence: How our Past Became Classical and the Future Turned Quantum. *Chem. Phys.* **2020**, 110663.
74. Irgen-Gioro, S.; Gururangan, K.; Saer, R.G.; Blankenship, R.E.; Harel, E. Electronic coherence lifetimes of the Fenna–Matthews–Olson complex and light harvesting complex II. *Chem. Sci.* **2019**, *10*, 10503–10509. [CrossRef] [PubMed]
75. Barroso-Flores, J. Evolution of the Fenna–Matthews–Olson Complex and Its Quantum Coherence Features. Which Led the Way? *ACS Cent. Sci.* **2017**, *3*, 1061–1062. [CrossRef] [PubMed]
76. Scholes, G.D.; Fleming, G.R.; Chen, L.X.; Aspuru-Guzik, A.; Buchleitner, A.; Coker, D.F.; Engel, G.S.; Van Grondelle, R.; Ishizaki, A.; Jonas, D.M.; et al. Using coherence to enhance function in chemical and biophysical systems. *Nature* **2017**, *543*, 647–656. [CrossRef]
77. Bai, S.; Song, K.; Shi, Q. Effects of Different Quantum Coherence on the Pump-Probe Polarization Anisotropy of Photosynthetic Light-Harvesting Complexes: A Computational Study. *J. Phys. Chem. Lett.* **2015**, *6*, 1954–1960. [CrossRef]
78. Song, K.; Bai, S.; Shi, Q. Effect of Pulse Shaping on Observing Coherent Energy Transfer in Single Light-Harvesting Complexes. *J. Phys. Chem. B* **2016**, *120*, 11637–11643. [CrossRef]
79. Chen, G.Y.; Lambert, N.; Shih, Y.A.; Liu, M.H.; Chen, Y.N.; Nori, F. Plasmonic bio-sensing for the Fenna-Matthews-Olson complex. *Sci. Rep.* **2017**, *7*, 39720. [CrossRef]
80. Lee, M.K.; Coker, D.F. Modeling Electronic-Nuclear Interactions for Excitation Energy Transfer Processes in Light-Harvesting Complexes. *J. Phys. Chem. Lett.* **2016**, *7*, 3171–3178. [CrossRef]
81. Olbrich, C.; Kleinekathöfer, U. Time-Dependent Atomistic View on the Electronic Relaxation in Light-Harvesting System II. *J. Phys. Chem. B* **2010**, *114*, 12427–12437. [CrossRef]
82. Olbrich, C.; Jansen, T.L.C.; Liebers, J.; Aghtar, M.; Strümpfer, J.; Schulten, K.; Knoester, J.; Kleinekathöfer, U. From Atomistic Modeling to Excitation Transfer and Two-Dimensional Spectra of the FMO Light-Harvesting Complex. *J. Phys. Chem. B* **2011**, *115*, 8609–8621. [CrossRef]
83. Reimers, J.R.; Biczysko, M.; Bruce, D.; Coker, D.F.; Frankcombe, T.J.; Hashimoto, H.; Hauer, J.; Jankowiak, R.; Kramer, T.; Linnanto, J.; et al. Challenges facing an understanding of the nature of low-energy excited states in photosynthesis. *Biochim. Biophys. Acta (BBA)-Bioenerg.* **2016**, *1857*, 1627–1640. [CrossRef] [PubMed]

84. Ashbrook, S.E.; Sneddon, S. New methods and applications in solid-state NMR spectroscopy of quadrupolar nuclei. *J. Am. Chem. Soc.* **2014**, *136*, 15440–15456. [CrossRef] [PubMed]
85. Pandit, A.; de Groot, H.J. Solid-state NMR applied to photosynthetic light-harvesting complexes. *Photosynth. Res.* **2012**, *111*, 219–226. [CrossRef] [PubMed]
86. Facelli, J.C. Chemical shift tensors: Theory and application to molecular structural problems. *Prog. Nucl. Magn. Reson. Spectrosc.* **2011**, *58*, 176–201. [CrossRef] [PubMed]
87. Man, P.P. Quadrupolar Interactions. In *Encyclopedia of Magnetic Resonance*; Grant, D.M., Harris, R.K., Eds.; John Wiley & Sons, Ltd.: Hoboken, NJ, USA, 1996; pp. 3838–3846.
88. Sarovar, M.; Ishizaki, A.; Fleming, G.R.; Whaley, K.B. Quantum entanglement in photosynthetic light-harvesting complexes. *Nat. Phys.* **2010**, *6*, 462–467. [CrossRef]
89. Zhu, J.; Kais, S.; Aspuru-Guzik, A.; Rodriques, S.; Brock, B.; Love, P.J. Multipartite quantum entanglement evolution in photosynthetic complexes. *J. Chem. Phys.* **2012**, *137*, 074112. [CrossRef]
90. Bardeen, C.J. Time dependent correlations of entangled states with nondegenerate branches and possible experimental realization using singlet fission. *J. Chem. Phys.* **2019**, *151*, 124503. [CrossRef]
91. Bengtsson, I.; Zyczkowski, K. *Geometry of Quantum States: An Introduction to Quantum Entanglement*; Cambridge University Press: Cambridge, UK, 2007.
92. Singh, D.; Dasgupta, S. Coherence and Its Role in Excitation Energy Transfer in Fenna–Matthews–Olson Complex. *J. Phys. Chem. B* **2017**, *121*, 1290–1294. [CrossRef]
93. Panitchayangkoon, G.; Voronine, D.V.; Abramavicius, D.; Caram, J.R.; Lewis, N.H.; Mukamel, S.; Engel, G.S. Direct evidence of quantum transport in photosynthetic light-harvesting complexes. *Proc. Natl. Acad. Sci. USA* **2011**, *108*, 20908–20912. [CrossRef]
94. Kell, A.; Khmelnitskiy, A.Y.; Reinot, T.; Jankowiak, R. On uncorrelated inter-monomer Förster energy transfer in Fenna–Matthews–Olson complexes. *J. R. Soc. Interface* **2019**, *16*, 20180882. [CrossRef]
95. Streltsov, A.; Adesso, G.; Plenio, M.B. Colloquium: Quantum coherence as a resource. *Rev. Mod. Phys.* **2017**, *89*, 041003. [CrossRef]
96. Wilkins, D.M.; Dattani, N.S. Why Quantum Coherence Is Not Important in the Fenna–Matthews–Olsen Complex. *J. Chem. Theory Comput.* **2015**, *11*, 3411–3419. [CrossRef] [PubMed]
97. Keren, N.; Paltiel, Y. Photosynthetic energy transfer at the quantum/classical border. *Trends Plant Sci.* **2018**, *23*, 497–506. [CrossRef] [PubMed]
98. Ishizaki, A.; Fleming, G.R. On the adequacy of the Redfield equation and related approaches to the study of quantum dynamics in electronic energy transfer. *J. Chem. Phys.* **2009**, *130*, 234110. [CrossRef] [PubMed]
99. Ishizaki, A.; Fleming, G.R. Unified treatment of quantum coherent and incoherent hopping dynamics in electronic energy transfer: Reduced hierarchy equation approach. *J. Chem. Phys.* **2009**, *130*, 234111. [CrossRef]
100. Tanimura, Y. Numerically "exact" approach to open quantum dynamics: The hierarchical equations of motion (HEOM). *J. Chem. Phys.* **2020**, *153*, 020901. [CrossRef]
101. Hein, B.; Kreisbeck, C.; Kramer, T.; Rodríguez, M. Modelling of oscillations in two-dimensional echo-spectra of the Fenna–Matthews–Olson complex. *New J. Phys.* **2012**, *14*, 023018. [CrossRef]
102. Chen, H.B.; Lambert, N.; Cheng, Y.C.; Chen, Y.N.; Nori, F. Using non-Markovian measures to evaluate quantum master equations for photosynthesis. *Sci. Rep.* **2015**, *5*, 12753. [CrossRef]
103. Kell, A.; Blankenship, R.E.; Jankowiak, R. Effect of Spectral Density Shapes on the Excitonic Structure and Dynamics of the Fenna–Matthews–Olson Trimer from Chlorobaculum tepidum. *J. Phys. Chem. A* **2016**, *120*, 6146–6154. [CrossRef]
104. Zhu, J.; Kais, S.; Rebentrost, P.; Aspuru-Guzik, A. Modified scaled hierarchical equation of motion approach for the study of quantum coherence in photosynthetic complexes. *J. Phys. Chem. B* **2011**, *115*, 1531–1537. [CrossRef]
105. Vulto, S.I.; Neerken, S.; Louwe, R.J.; de Baat, M.A.; Amesz, J.; Aartsma, T.J. Excited-state structure and dynamics in FMO antenna complexes from photosynthetic green sulfur bacteria. *J. Phys. Chem. B* **1998**, *102*, 10630–10635. [CrossRef]
106. Vulto, S.I.; de Baat, M.A.; Louwe, R.J.; Permentier, H.P.; Neef, T.; Miller, M.; van Amerongen, H.; Aartsma, T.J. Exciton simulations of optical spectra of the FMO complex from the green sulfur bacterium Chlorobium tepidum at 6 K. *J. Phys. Chem. B* **1998**, *102*, 9577–9582. [CrossRef]

107. Vulto, S.I.E.; de Baat, M.A.; Neerken, S.; Nowak, F.R.; van Amerongen, H.; Amesz, J.; Aartsma, T.J. Excited State Dynamics in FMO Antenna Complexes from Photosynthetic Green Sulfur Bacteria: A Kinetic Model. *J. Phys. Chem. B* **1999**, *103*, 8153–8161. [CrossRef]
108. Adolphs, J.; Müh, F.; Madjet, M.E.A.; Renger, T. Calculation of pigment transition energies in the FMO protein. *Photosynth. Res.* **2008**, *95*, 197. [CrossRef]
109. Gao, J.; Shi, W.J.; Ye, J.; Wang, X.; Hirao, H.; Zhao, Y. QM/MM Modeling of Environmental Effects on Electronic Transitions of the FMO Complex. *J. Phys. Chem. B* **2013**, *117*, 3488–3495. [CrossRef]
110. Tian, B.L.; Ding, J.J.; Xu, R.X.; Yan, Y. Biexponential theory of Drude dissipation via hierarchical quantum master equation. *J. Chem. Phys.* **2010**, *133*, 114112. [CrossRef]
111. Renger, T.; Müh, F. Theory of excitonic couplings in dielectric media. *Photosynth. Res.* **2012**, *111*, 47–52. [CrossRef]
112. Madjet, M.E.; Abdurahman, A.; Renger, T. Intermolecular Coulomb Couplings from Ab Initio Electrostatic Potentials: Application to Optical Transitions of Strongly Coupled Pigments in Photosynthetic Antennae and Reaction Centers. *J. Phys. Chem. B* **2006**, *110*, 17268–17281. [CrossRef]
113. Cupellini, L.; Jurinovich, S.; Campetella, M.; Caprasecca, S.; Guido, C.A.; Kelly, S.M.; Gardiner, A.T.; Cogdell, R.; Mennucci, B. An Ab Initio Description of the Excitonic Properties of LH2 and Their Temperature Dependence. *J. Phys. Chem. B* **2016**, *120*, 11348–11359.
114. Aghtar, M.; Kleinekathöfer, U.; Curutchet, C.; Mennucci, B. Impact of Electronic Fluctuations and Their Description on the Exciton Dynamics in the Light-Harvesting Complex PE545. *J. Phys. Chem. B* **2017**, *121*, 1330–1339. [CrossRef]
115. Cole, D.J.; Hine, N.D.M. Applications of large-scale density functional theory in biology. *J. Phys. Condens. Matter* **2016**, *28*, 393001. [CrossRef] [PubMed]
116. Pinheiro, S.; Curutchet, C. Can Förster Theory Describe Stereoselective Energy Transfer Dynamics in a Protein–Ligand Complex? *J. Phys. Chem. B* **2017**, *121*, 2265–2278. [CrossRef] [PubMed]
117. Lewis, N.H.C.; Gruenke, N.L.; Oliver, T.A.A.; Ballottari, M.; Bassi, R.; Fleming, G.R. Observation of Electronic Excitation Transfer Through Light Harvesting Complex II Using Two-Dimensional Electronic-Vibrational Spectroscopy. *J. Phys. Chem. Lett.* **2016**, *7*, 4197–4206. [CrossRef]
118. Stratmann, R.E.; Scuseria, G.E. An efficient implementation of time-dependent density-functional theory for the calculation of excitation energies of large molecules. *J. Chem. Phys.* **1998**, *109*, 8218–8224. [CrossRef]
119. Petersilka, M.; Gossmann, U.J.; Gross, E.K.U. Excitation Energies from Time-Dependent Density-Functional Theory. *Phys. Rev. Lett.* **1996**, *76*, 1212–1215. [CrossRef]
120. Dreuw, A.; Weisman, J.L.; Head-Gordon, M. Long-range charge-transfer excited states in time-dependent density functional theory require non-local exchange. *J. Chem. Phys.* **2003**, *119*, 2943–2946. [CrossRef]
121. Tawada, Y.; Tsuneda, T.; Yanagisawa, S.; Yanai, T.; Hirao, K. A long-range-corrected time-dependent density functional theory. *J. Chem. Phys.* **2004**, *120*, 8425–8433. [CrossRef]
122. Chong, D.P. *Recent Advances in Density Functional Methods: (Part I)*; World Scientific: Singapore, 1995.
123. Gross, E.K.U.; Kohn, W. Time-Dependent Density-Functional Theory. In *Advances in Quantum Chemistry*; Löwdin, P.O., Ed.; Academic Press: Cambridge, MA, USA,1990; Volume 21, pp. 255–291.
124. Badu, S.; Melnik, R. NMR properties of Fenna–Matthews–Olson light harvesting complex: Photosynthesis and its biomedical applications. In Proceedings of the 2017 IEEE First, Ukraine Conference on Electrical and Computer Engineering (UKRCON), Kyiv, Ukraine, 29 May–2 June 2017; IEEE: Piscataway, NJ, USA, 2017; pp. 318–321.
125. Badu, S.; Prabhakar, S.; Melnik, R. Component spectroscopic properties of light-harvesting complexes with DFT calculations. *Biocell* **2020**, *44*, 279–291. [CrossRef]
126. Badu, S.; Melnik, R.; Prabhakar, S. Photosynthesis and electronic properties of Fenna-Mathhews-Olson light harvesting complexes. Proceedings and Extended Abstracts. In Proceedings of the IWBBIO 2016 International Work-Conference on Bioinformatics and Biomedical Engineering, IWBBIO 2016, Granada, Spain, 20–22 April 2016; pp. 202–203.
127. Frisch, M.; Trucks, G.W.; Schlegel, H.B.; Scuseria, G.E.; Robb, M.A.; Cheeseman, J.R.; Scalmani, G.; Barone, V.; Mennucci, B.; Petersson, G.E.; et al. *Gaussian 09 Revision D. 01*; Inc.: Wallingford, CT, USA, 2014.
128. Adamo, C.; Barone, V. Toward reliable density functional methods without adjustable parameters: The PBE0 model. *J. Chem. Phys.* **1999**, *110*, 6158–6170. [CrossRef]

129. Perdew, J.P.; Burke, K.; Ernzerhof, M. Generalized Gradient Approximation Made Simple. *Phys. Rev. Lett.* **1996**, *77*, 3865–3868. [CrossRef]
130. Perdew, J.P.; Burke, K.; Ernzerhof, M. Reply to Comment on generalized gradient approximation made simple. *Phys. Rev. Lett.* **1998**, *80*, 891. [CrossRef]
131. Humphrey, W.; Dalke, A.; Schulten, K. VMD: Visual molecular dynamics. *J. Mol. Graph.* **1996**, *14*, 33–38. [CrossRef]
132. Khmelnitskiy, A.; Reinot, T.; Jankowiak, R. Impact of Single-Point Mutations on the Excitonic Structure and Dynamics in a Fenna–Matthews–Olson Complex. *J. Phys. Chem. Lett.* **2018**, *9*, 3378–3386. [CrossRef] [PubMed]
133. Chandrasekaran, S.; Aghtar, M.; Valleau, S.; Aspuru-Guzik, A.; Kleinekathöfer, U. Influence of Force Fields and Quantum Chemistry Approach on Spectral Densities of BChl a in Solution and in FMO Proteins. *J. Phys. Chem. B* **2015**, *119*, 9995–10004. [CrossRef] [PubMed]
134. Jurinovich, S.; Viani, L.; Curutchet, C.; Mennucci, B. Limits and potentials of quantum chemical methods in modelling photosynthetic antennae. *Phys. Chem. Chem. Phys.* **2015**, *17*, 30783–30792. [CrossRef]
135. Aghtar, M.; Kleinekathöfer, U. Environmental coupling and population dynamics in the PE545 light-harvesting complex. *J. Lumin.* **2016**, *169, Part B*, 406–409. [CrossRef]
136. Zheng, F.; Jin, M.; Mancal, T.; Zhao, Y. Study of Electronic Structures and Pigment-Protein Interactions in the Reaction Center of Thermochromatium tepidum with a Dynamic Environment. *J. Phys. Chem. B* **2016**, *120*, 10046–10058. [CrossRef]
137. Jankowiak, R.; Reppert, M.; Zazubovich, V.; Pieper, J.; Reinot, T. Site selective and single complex laser-based spectroscopies: A window on excited state electronic structure, excitation energy transfer, and electron–phonon coupling of selected photosynthetic complexes. *Chem. Rev.* **2011**, *111*, 4546–4598. [CrossRef]
138. Kramer, T.; Rodríguez, M. Effect of disorder and polarization sequences on two-dimensional spectra of light-harvesting complexes. *Photosynth. Res.* **2019**, 1–8. [CrossRef]
139. Engel, G.S.; Calhoun, T.R.; Read, E.L.; Ahn, T.K.; Mančal, T.; Cheng, Y.C.; Blankenship, R.E.; Fleming, G.R. Evidence for wavelike energy transfer through quantum coherence in photosynthetic systems. *Nature* **2007**, *446*, 782–786. [CrossRef]
140. Lambrev, P.H.; Akhtar, P.; Tan, H.S. Insights into the mechanisms and dynamics of energy transfer in plant light-harvesting complexes from two-dimensional electronic spectroscopy. *Biochim. Biophys. Acta (BBA)-Bioenerg.* **2019**. [CrossRef] [PubMed]
141. Claridge, K.; Padula, D.; Troisi, A. On the arrangement of chromophores in light harvesting complexes: chance versus design. *Faraday Discuss.* **2019**, *221*, 133–149. [CrossRef] [PubMed]
142. Gururangan, K.; Harel, E. Coherent and dissipative quantum process tensor reconstructions in two-dimensional electronic spectroscopy. *J. Chem. Phys.* **2019**, *150*, 164127. [CrossRef] [PubMed]
143. Badu, S.; Melnik, R. Fundamental molecular complexes of photosynthesis and their biomedical applications. In Proceedings of the IWBBIO 2017 International Work-Conference on Bioinformatics and Biomedical Engineering, IWBBIO 2017, Granada, Spain, 26–28 April 2017; pp. 94–96.
144. Croce, R.; van Grondelle, R.; van Amerongen, H.; van Stokkum, I. *Light Harvesting in Photosynthesis*; CRC Press: Boca Raton, FL, USA, 2018.
145. Halder, P.; Azad, A. Recent trends and challenges of algal biofuel conversion technologies. In *Advanced Biofuels*; Elsevier: Amsterdam, The Netherlands, 2019; pp. 167–179.
146. Syrpas, M.; Venskutonis, P.R. Algae for the production of bio-based products. In *Biobased Products and Industries*; Elsevier: Amsterdam, The Netherlands, 2020; pp. 203–243.
147. Kumar, M.; Sun, Y.; Rathour, R.; Pandey, A.; Thakur, I.S.; Tsang, D.C. Algae as potential feedstock for the production of biofuels and value-added products: Opportunities and challenges. *Sci. Total. Environ.* **2020**, *716*, 137116. [CrossRef] [PubMed]
148. Veeramuthu, A.; Ngamcharussrivichai, C. Potential of microalgal biodiesel: Challenges and applications. In *Renewable Energy*; IntechOpen: London, UK, 2020.
149. Hitchcock, A.; Hunter, C.N.; Canniffe, D.P. Progress and challenges in engineering cyanobacteria as chassis for light-driven biotechnology. *Microb. Biotechnol.* **2020**, *13*, 363–367. [CrossRef]

150. Khan, A.Z.; Bilal, M.; Mehmood, S.; Sharma, A.; Iqbal, H. State-of-the-Art Genetic Modalities to Engineer Cyanobacteria for Sustainable Biosynthesis of Biofuel and Fine-Chemicals to Meet Bio–Economy Challenges. *Life* **2019**, *9*, 54. [CrossRef]
151. Zhang, Y.; Liu, M.; Zhou, M.; Yang, H.; Liang, L.; Gu, T. Microbial fuel cell hybrid systems for wastewater treatment and bioenergy production: Synergistic effects, mechanisms and challenges. *Renew. Sustain. Energy Rev.* **2019**, *103*, 13–29. [CrossRef]
152. Gul, M.M.; Ahmad, K.S. Bioelectrochemical systems: Sustainable bio-energy powerhouses. *Biosens. Bioelectron.* **2019**, *142*, 111576. [CrossRef]
153. Mouhib, M.; Antonucci, A.; Reggente, M.; Amirjani, A.; Gillen, A.J.; Boghossian, A.A. Enhancing bioelectricity generation in microbial fuel cells and biophotovoltaics using nanomaterials. *Nano Res.* **2019**, *12*, 2184–2199. [CrossRef]
154. ElMekawy, A.; Hegab, H.M.; Vanbroekhoven, K.; Pant, D. Techno-productive potential of photosynthetic microbial fuel cells through different configurations. *Renew. Sustain. Energy Rev.* **2014**, *39*, 617–627. [CrossRef]
155. Qi, X.; Ren, Y.; Liang, P.; Wang, X. New insights in photosynthetic microbial fuel cell using anoxygenic phototrophic bacteria. *Bioresour. Technol.* **2018**, *258*, 310–317. [CrossRef] [PubMed]
156. Xu, H.; Wang, L.; Wen, Q.; Chen, Y.; Qi, L.; Huang, J.; Tang, Z. A 3D porous NCNT sponge anode modified with chitosan and Polyaniline for high-performance microbial fuel cell. *Bioelectrochemistry* **2019**, *129*, 144–153. [CrossRef]
157. Milano, F.; Punzi, A.; Ragni, R.; Trotta, M.; Farinola, G.M. Photonics and optoelectronics with bacteria: Making materials from photosynthetic microorganisms. *Adv. Funct. Mater.* **2019**, *29*, 1805521. [CrossRef]
158. Di Lauro, M.; la Gatta, S.; Bortolotti, C.A.; Beni, V.; Parkula, V.; Drakopoulou, S.; Giordani, M.; Berto, M.; Milano, F.; Cramer, T.; et al. A Bacterial Photosynthetic Enzymatic Unit Modulating Organic Transistors with Light. *Adv. Electron. Mater.* **2020**, *6*, 1900888. [CrossRef]
159. Sun, J.; Yang, P.; Li, N.; Zhao, M.; Zhang, X.; Zhang, Y.; Yuan, Y.; Lu, X.; Lu, X. Extraction of photosynthetic electron from mixed photosynthetic consortium of bacteria and algae towards sustainable bioelectrical energy harvesting. *Electrochim. Acta* **2020**, *336*, 135710. [CrossRef]
160. McKendry, P. Energy production from biomass (part 1): Overview of biomass. *Bioresour. Technol.* **2002**, *83*, 37–46. [CrossRef]
161. Cruz, J.A.; Avenson, T.J.; Kanazawa, A.; Takizawa, K.; Edwards, G.E.; Kramer, D.M. Plasticity in light reactions of photosynthesis for energy production and photoprotection. *J. Exp. Bot.* **2005**, *56*, 395–406. [CrossRef]
162. Walker, B.J.; Kramer, D.M.; Fisher, N.; Fu, X. Flexibility in the Energy Balancing Network of Photosynthesis Enables Safe Operation under Changing Environmental Conditions. *Plants* **2020**, *9*, 301. [CrossRef]
163. Dimitriev, O.; Yoshida, T.; Sun, H. Principles of solar energy storage. *Energy Storage* **2020**, *2*, e96. [CrossRef]
164. Ravi, S.K.; Rawding, P.; Elshahawy, A.M.; Huang, K.; Sun, W.; Zhao, F.; Wang, J.; Jones, M.R.; Tan, S.C. Photosynthetic apparatus of Rhodobacter sphaeroides exhibits prolonged charge storage. *Nat. Commun.* **2019**, *10*, 1–10. [CrossRef]
165. Liu, Y.; Ge, Z.; Sun, Z.; Zhang, Y.; Dong, C.; Zhang, M.; Li, Z.; Chen, Y. A high-performance energy storage system from sphagnum uptake waste LIBs with negative greenhouse-gas emission. *Nano Energy* **2020**, *67*, 104216. [CrossRef]
166. Zhou, Q.; Zhang, P.; Zhang, G. Biomass and pigments production in photosynthetic bacteria wastewater treatment: Effects of light sources. *Bioresour. Technol.* **2015**, *179*, 505–509. [CrossRef] [PubMed]
167. Abinandan, S.; Shanthakumar, S. Challenges and opportunities in application of microalgae (Chlorophyta) for wastewater treatment: A review. *Renew. Sustain. Energy Rev.* **2015**, *52*, 123–132. [CrossRef]
168. Liu, J.; Pemberton, B.; Lewis, J.; Scales, P.J.; Martin, G.J. Wastewater treatment using filamentous algae—A review. *Bioresour. Technol.* **2019**, 122556. [CrossRef] [PubMed]
169. Umar, L.; Alexander, F.A.; Wiest, J. Application of algae-biosensor for environmental monitoring. In Proceedings of the 2015 37th Annual International Conference of the IEEE Engineering in Medicine and Biology Society (EMBC), Milano, Italy, 25–29 August 2015; pp. 7099–7102.
170. Wati, A.; Rusva, R.; Umar, L. Effect of LED Wavelengths and Light-Dark Cycle on Photosynthetic Production of Chlorella Kessleri for Algae-Based Biosensor Optimization. In *Journal of Physics: Conference Series*; IOP Publishing: Bristol, UK, 2019; Volume 1351, p. 012003.

171. Umar, L.; Hamzah, Y.; Setiadi, R.N. Biosensor signal improvement using current mirror topology for dissolved oxygen measurement. *Meas. Sci. Technol.* **2019**, *30*, 065102. [CrossRef]
172. Xu, M.; Melnik, R.V.; Borup, U. Modeling anti-islanding protection devices for photovoltaic systems. *Renew. Energy* **2004**, *29*, 2195–2216. [CrossRef]
173. Alharbi, F.H.; Kais, S. Theoretical limits of photovoltaics efficiency and possible improvements by intuitive approaches learned from photosynthesis and quantum coherence. *Renew. Sustain. Energy Rev.* **2015**, *43*, 1073–1089. [CrossRef]
174. Brédas, J.L.; Sargent, E.H.; Scholes, G.D. Photovoltaic concepts inspired by coherence effects in photosynthetic systems. *Nat. Mater.* **2017**, *16*, 35–44. [CrossRef]
175. Romero, E.; Novoderezhkin, V.I.; van Grondelle, R. Quantum design of photosynthesis for bio-inspired solar-energy conversion. *Nature* **2017**, *543*, 355–365. [CrossRef]
176. Dong, Y.; Cha, H.; Zhang, J.; Pastor, E.; Tuladhar, P.S.; McCulloch, I.; Durrant, J.R.; Bakulin, A.A. The binding energy and dynamics of charge-transfer states in organic photovoltaics with low driving force for charge separation. *J. Chem. Phys.* **2019**, *150*, 104704. [CrossRef]
177. Gasparini, N.; Salleo, A.; McCulloch, I.; Baran, D. The role of the third component in ternary organic solar cells. *Nat. Rev. Mater.* **2019**, *4*, 229–242. [CrossRef]
178. Segev, G.; Beeman, J.W.; Greenblatt, J.B.; Sharp, I.D. Hybrid photoelectrochemical and photovoltaic cells for simultaneous production of chemical fuels and electrical power. *Nat. Mater.* **2018**, *17*, 1115–1121. [CrossRef] [PubMed]
179. Gelbwaser-Klimovsky, D.; Aspuru-Guzik, A. On thermodynamic inconsistencies in several photosynthetic and solar cell models and how to fix them. *Chem. Sci.* **2017**, *8*, 1008–1014. [CrossRef] [PubMed]
180. Han, G.; Yi, Y.; Shuai, Z. From molecular packing structures to electronic processes: theoretical simulations for organic solar cells. *Adv. Energy Mater.* **2018**, *8*, 1702743. [CrossRef]
181. Zhao, Z.W.; Pan, Q.Q.; Geng, Y.; Wu, S.X.; Zhang, M.; Zhao, L.; Su, Z.M. A theorectical design of performant chlorinated benzothiadiazole-based polymers as donor for organic photovoltaic devices. *Org. Electron.* **2018**, *61*, 46–55. [CrossRef]
182. Nelson, T.R.; White, A.J.; Bjorgaard, J.A.; Sifain, A.E.; Zhang, Y.; Nebgen, B.; Fernandez-Alberti, S.; Mozyrsky, D.; Roitberg, A.E.; Tretiak, S. Non-adiabatic Excited-State Molecular Dynamics: Theory and Applications for Modeling Photophysics in Extended Molecular Materials. *Chem. Rev.* **2020**, *120*, 2215–2287. [CrossRef]
183. Schröder, F.A.; Turban, D.H.; Musser, A.J.; Hine, N.D.; Chin, A.W. Tensor network simulation of multi-environmental open quantum dynamics via machine learning and entanglement renormalisation. *Nat. Commun.* **2019**, *10*, 1–10. [CrossRef]
184. Zhao, Z.W.; Pan, Q.Q.; Geng, Y.; Wu, Y.; Zhao, L.; Zhang, M.; Su, Z.M. Theoretical Insight into Multiple Charge-Transfer Mechanisms at the P3HT/Nonfullerenes Interface in Organic Solar Cells. *ACS Sustain. Chem. Eng.* **2019**, *7*, 19699–19707. [CrossRef]
185. Marmolejo-Valencia, A.F.; Mata-Pinzón, Z.; Dominguez, L.; Amador-Bedolla, C. Atomistic simulations of bulk heterojunctions to evaluate the structural and packing properties of new predicted donors in OPVs. *Phys. Chem. Chem. Phys.* **2019**, *21*, 20315–20326. [CrossRef]
186. Bonke, S.A.; Wiechen, M.; MacFarlane, D.R.; Spiccia, L. Renewable fuels from concentrated solar power: Towards practical artificial photosynthesis. *Energy Environ. Sci.* **2015**, *8*, 2791–2796. [CrossRef]
187. Fukuzumi, S. Artificial photosynthesis for production of hydrogen peroxide and its fuel cells. *Biochim. Biophys. Acta (BBA)-Bioenerg.* **2016**, *1857*, 604–611. [CrossRef] [PubMed]
188. Gamba, I. Biomimetic Approach to CO_2 Reduction. *Bioinorg. Chem. Appl.* **2018**, *2379141*. [CrossRef] [PubMed]
189. Zhou, H.; Li, P.; Liu, J.; Chen, Z.; Liu, L.; Dontsova, D.; Yan, R.; Fan, T.; Zhang, D.; Ye, J. Biomimetic polymeric semiconductor based hybrid nanosystems for artificial photosynthesis towards solar fuels generation via CO_2 reduction. *Nano Energy* **2016**, *25*, 128–135. [CrossRef]
190. Quader, M.; Ahmed, S. Bioenergy with carbon capture and storage (BECCS): Future prospects of carbon-negative technologies. In *Clean Energy for Sustainable Development*; Elsevier: Amsterdam, The Netherlands, 2017; pp. 91–140.
191. Barber, J. Photosynthetic energy conversion: Natural and artificial. *Chem. Soc. Rev.* **2009**, *38*, 185–196. [CrossRef] [PubMed]

192. Kay, A.; Graetzel, M. Artificial photosynthesis. 1. Photosensitization of titania solar cells with chlorophyll derivatives and related natural porphyrins. *J. Phys. Chem.* **1993**, *97*, 6272–6277. [CrossRef]
193. Berardi, S.; Drouet, S.; Francas, L.; Gimbert-Suriñach, C.; Guttentag, M.; Richmond, C.; Stoll, T.; Llobet, A. Molecular artificial photosynthesis. *Chem. Soc. Rev.* **2014**, *43*, 7501–7519. [CrossRef]
194. Fukuzumi, S.; Ohkubo, K.; Suenobu, T. Long-Lived Charge Separation and Applications in Artificial Photosynthesis. *Acc. Chem. Res.* **2014**, *47*, 1455–1464. [CrossRef]
195. Kim, D.; Sakimoto, K.K.; Hong, D.; Yang, P. Artificial Photosynthesis for Sustainable Fuel and Chemical Production. *Angew. Chem. Int. Ed.* **2015**, *54*, 3259–3266. [CrossRef]
196. Faunce, T.; Styring, S.; Wasielewski, M.R.; Brudvig, G.W.; Rutherford, A.W.; Messinger, J.; Lee, A.F.; Hill, C.L.; Degroot, H.; Fontecave, M.; et al. Artificial photosynthesis as a frontier technology for energy sustainability. *Energy Environ. Sci.* **2013**, *6*, 1074–1076. [CrossRef]
197. Mora, S.J.; Odella, E.; Moore, G.F.; Gust, D.; Moore, T.A.; Moore, A.L. Proton-Coupled Electron Transfer in Artificial Photosynthetic Systems. *Accounts Chem. Res.* **2018**, *51*, 445–453. [CrossRef]
198. Odella, E.; Mora, S.J.; Wadsworth, B.L.; Huynh, M.T.; Goings, J.J.; Liddell, P.A.; Groy, T.L.; Gervaldo, M.; Sereno, L.E.; Gust, D.; et al. Controlling proton-coupled electron transfer in bioinspired artificial photosynthetic relays. *J. Am. Chem. Soc.* **2018**, *140*, 15450–15460. [CrossRef] [PubMed]
199. Brown, K.A.; King, P.W. Coupling biology to synthetic nanomaterials for semi-artificial photosynthesis. *Photosynth. Res.* **2019**, 1–11. [CrossRef] [PubMed]
200. Berhanu, S.; Ueda, T.; Kuruma, Y. Artificial photosynthetic cell producing energy for protein synthesis. *Nat. Commun.* **2019**, *10*, 1–10. [CrossRef]
201. Lee, K.Y.; Park, S.J.; Lee, K.A.; Kim, S.H.; Kim, H.; Meroz, Y.; Mahadevan, L.; Jung, K.H.; Ahn, T.K.; Parker, K.K.; et al. Photosynthetic artificial organelles sustain and control ATP-dependent reactions in a protocellular system. *Nat. Biotechnol.* **2018**, *36*, 530–535. [CrossRef]
202. Lee, Y.V.; Tian, B. Learning from Solar Energy Conversion: Biointerfaces for Artificial Photosynthesis and Biological Modulation. *Nano Lett.* **2019**, *19*, 2189–2197. [CrossRef] [PubMed]
203. Bruce, A.; Faunce, T. Sustainable fuel, food, fertilizer and ecosystems through a global artificial photosynthetic system: Overcoming anticompetitive barriers. *Interface Focus* **2015**, *5*, 20150011. [CrossRef]
204. Long, S.P.; Zhu, X.G.; Naidu, S.L.; Ort, D.R. Can improvement in photosynthesis increase crop yields? *Plant Cell Environ.* **2006**, *29*, 315–330. [CrossRef]
205. Borg, O.A.; Godinho, S.S.; Lundqvist, M.J.; Lunell, S.; Persson, P. Computational study of the lowest triplet state of ruthenium polypyridyl complexes used in artificial photosynthesis. *J. Phys. Chem. A* **2008**, *112*, 4470–4476. [CrossRef]
206. Barber, J.; Tran, P.D. From natural to artificial photosynthesis. *J. R. Soc. Interface* **2013**, *10*, 20120984. [CrossRef]
207. Asahi, R.; Jinnouchi, R. Atomistic modeling of photoelectric cells for artificial photosynthesis. *Multiscale Simul. Electrochem. Devices* **2020**, *107*. [CrossRef]
208. Aitchison, C.M.; Andrei, V.; Antón-García, D.; Apfel, U.P.; Badiani, V.; Beller, M.; Bocarsly, A.B.; Bonnet, S.; Brueggeller, P.; Caputo, C.A.; et al. Synthetic approaches to artificial photosynthesis: General discussion. *Faraday Discuss.* **2019**, *215*, 242–281. [CrossRef] [PubMed]
209. Darensbourg, M.Y.; Llobet, A. Preface for Small Molecule Activation: From Biological Principles to Energy Applications. Part 3: Small Molecules Related to (Artificial) Photosynthesis. *Inorg. Chem.* **2016**, *55*, 371–377. [CrossRef]
210. Guiglion, P.; Berardo, E.; Butchosa, C.; Wobbe, M.C.C.; Zwijnenburg, M.A. Modelling materials for solar fuel synthesis by artificial photosynthesis; predicting the optical, electronic and redox properties of photocatalysts. *J. Phys. Condens. Matter* **2016**, *28*, 074001. [CrossRef] [PubMed]
211. Pann, J.; Roithmeyer, H.; Viertl, W.; Pehn, R.; Bendig, M.; Dutzler, J.; Kriesche, B.; Brüggeller, P. Phosphines in artificial photosynthesis: Considering different aspects such as chromophores, water reduction catalysts (WRCs), water oxidation catalysts (WOCs), and dyads. *Sustain. Energy Fuels* **2019**, *3*, 2926–2953. [CrossRef]
212. Guiglion, P.; Monti, A.; Zwijnenburg, M.A. Validating a density functional theory approach for predicting the redox potentials associated with charge carriers and excitons in polymeric photocatalysts. *J. Phys. Chem. C* **2017**, *121*, 1498–1506. [CrossRef]
213. Shtarev, D.S.; Shtareva, A.V.; Ryabchuk, V.K.; Rudakova, A.V.; Serpone, N. Considerations of Trends in Heterogeneous Photocatalysis. Correlations between conduction and valence band energies with bandgap energies of various photocatalysts. *ChemCatChem* **2019**, *11*, 3534–3541. [CrossRef]

214. Wilbraham, L.; Sprick, R.S.; Jelfs, K.E.; Zwijnenburg, M.A. Mapping binary copolymer property space with neural networks. *Chem. Sci.* **2019**, *10*, 4973–4984. [CrossRef]
215. Zheng, G. Porphyrin Nanotechnology: Discovery, Clinical Translation and Beyond. In *Proceedings of the 2016 Asia Communications and Photonics Conference (ACP)*; IEEE: Piscataway, NJ, USA, 2016, pp. 1–3.
216. Ng, K.K.; Takada, M.; Harmatys, K.; Chen, J.; Zheng, G. Chlorosome-Inspired Synthesis of Templated Metallochlorin-Lipid Nanoassemblies for Biomedical Applications. *ACS Nano* **2016**, *10*, 4092–4101. [CrossRef]
217. Shao, S.; Rajendiran, V.; Lovell, J.F. Metalloporphyrin nanoparticles: Coordinating diverse theranostic functions. *Coord. Chem. Rev.* **2019**, *379*, 99–120. [CrossRef]
218. Mironov, A.F.; Zhdanova, K.A.; Natal'ya, A.B. Nanosized vehicles for delivery of photosensitizers in photodynamic diagnosis and therapy of cancer. *Russ. Chem. Rev.* **2018**, *87*, 859. [CrossRef]
219. MacLaughlin, J.A.; Anderson, R.R.; Holick, M.F. Spectral character of sunlight modulates photosynthesis of previtamin D3 and its photoisomers in human skin. *Science* **1982**, *216*, 1001–1003. [CrossRef] [PubMed]
220. Veronikis, A.J.; Cevik, M.B.; Allen, R.H.; Shirvani, A.; Sun, A.; Persons, K.S.; Holick, M.F. Evaluation of a Ultraviolet B Light Emitting Diode (LED) for Producing Vitamin D3 in Human Skin. *Anticancer Res.* **2020**, *40*, 719–722. [CrossRef] [PubMed]
221. Lambert, N.; Chen, Y.N.; Cheng, Y.C.; Li, C.M.; Chen, G.Y.; Nori, F. Quantum biology. *Nat. Phys.* **2013**, *9*, 10–18. [CrossRef]
222. Cupellini, L.; Bondanza, M.; Nottoli, M.; Mennucci, B. Successes & challenges in the atomistic modeling of light-harvesting and its photoregulation. *Biochim. Biophys. Acta (BBA)-Bioenerg.* **2020**, *1861*, 148049.
223. Lishchuk, A.; Vasilev, C.; Johnson, M.P.; Hunter, C.N.; Törmä, P.; Leggett, G.J. Turning the challenge of quantum biology on its head: Biological control of quantum optical systems. *Faraday Discuss.* **2019**, *216*, 57–71. [CrossRef] [PubMed]
224. Forn-Díaz, P.; Lamata, L.; Rico, E.; Kono, J.; Solano, E. Ultrastrong coupling regimes of light-matter interaction. *Rev. Mod. Phys.* **2019**, *91*, 025005. [CrossRef]
225. Wientjes, E.; Lambrev, P. Ultrafast processes in photosynthetic light-harvesting. *Photosynth. Res.* **2020**, *144*, 123–125. [CrossRef]
226. Duan, H.G.; Nalbach, P.; Miller, R.D.; Thorwart, M. Intramolecular vibrations enhance the quantum efficiency of excitonic energy transfer. *Photosynth. Res.* **2020**, 1–9. [CrossRef]